

**AN ANALYSIS OF THE SPRING-TO-SUMMER TRANSITION  
IN THE WEST CENTRAL MISSOURI PLAINS**

---

A Thesis presented to the Faculty of the Graduate School  
University of Missouri-Columbia

---

In Partial Fulfillment  
Of the Requirements for the Degree  
Master of Science

---

by  
ROSALIE NEWBERRY

Dr. Anthony Lupo, Thesis Supervisor

May, 2014

The undersigned, appointed by the dean of the Graduate School, have examined the thesis entitled

AN ANALYSIS OF THE SPRING-TO-SUMMER TRANSITION IN THE WEST  
CENTRAL MISSOURI PLAINS

presented by Rosalie Newberry,

a candidate for the degree of master of science,

and hereby certify that, in their opinion, it is worthy of acceptance.

---

Dr. Anthony Lupo, Professor

---

Dr. Neil Fox, Associate Professor

---

Dr. Stacey Woelfel, Associate Professor

## **ACKNOWLEDGEMENTS**

I would like to take this opportunity to thank my faculty at the University of Missouri, especially Dr. Anthony Lupo, Dr. Patrick Market and Dr. Neil Fox. Without their support, this project would have never been possible.

I would also like to thank the graduate students of Atmospheric Science, my peers, who gave me more aid than they realize.

An indebted thank-you goes to KOMU, the NBC Affiliate of Mid-Missouri, my employer. General Manager Marty Siddall and News Director Dr. Stacey Woelfel gifted me with unending flexibility and positivity through this degree process.

Dave Schmidt, Eric Aldrich and Michelle Bogowith taught me the essentials of weather communication; for that, I am grateful to them.

Finally, I'd like to thank my parents, Dr. Robin and Mrs. Mary Luke. I am forever appreciative of their love and compassion.

# TABLE OF CONTENTS

ACKNOWLEDGEMENTS .....	ii
LIST OF ILLUSTRATIONS .....	iv
ABSTRACT.....	vii
Chapter 1 INTRODUCTION .....	1
1.1 – PURPOSE .....	6
1.2 – OBJECTIVES .....	8
Chapter 2 DATA SELECTION METHODOLOGY.....	9
2.1 – TIME SERIES SELECTION .....	9
2.2 – LOCATION SELECTION .....	10
2.3 – DATA SELECTION .....	16
2.3.1 – OSCILLATION SELECTION.....	16
2.3.2 – UPPER-AIR MAP SELECTION.....	21
2.3.3 – STATISTICAL DATA SELECTION.....	25
2.3.4 – TEMPERATURE SELECTION.....	27
2.3.5 – PRECIPITATION SELECTION.....	27
2.3.6 – DATA ACCOUNTABILITY.....	28
Chapter 3 RESULTS AND ANALYSIS .....	30
3.1 – STUDY RESULTS.....	30
3.2 – DATA ANALYSIS .....	33
3.2.1 – OSCILLATION ANALYSIS.....	38
3.2.2 – UPPER-AIR MAPS ANALYSIS.....	46
3.2.3 – TEMPERATURE DATA ANALYSIS.....	51
3.2.4 – PRECIPITATION DATA ANALYSIS.....	55
3.2.5 – COMPARATIVE ANALYSIS.....	57
Chapter 4 CONCLUSIONS .....	65
Chapter 5 APPLICATIONS OF FINDINGS.....	68
Chapter 6 FURTHER STUDY.....	72
REFERENCES .....	74

# LIST OF ILLUSTRATIONS

<b>FIGURE</b>	<b>PAGE</b>
Figure 1.1 U.S. Tornado Averages by Month from 1991-2010, published by the National Climatic Data Center, a Division of the National Oceanic and Atmospheric Administration.....	2
Figure 2.1 Ratley et al. (2002) Location Selection, including Jefferson City, Missouri, 1981-2000. This area is bounded by the edge of the East Ozarks to the west, the Mississippi River to the east, the Missouri River to the north and the Missouri/Arkansas border to the south .....	11
Figure 2.2 United States Department of Commerce Weather Bureau’s “Climatological Data: Missouri Section,” Divisions, 1957 to Present .....	13
Figure 2.3 500-mb Height Map from the National Oceanic and Atmospheric Administration Central Library’s United States Daily Weather Maps Site. 19 June, 1968 .....	23
Figure 2.4 500-mb Height Map from the National Oceanic and Atmospheric Administration Central Library’s United States Daily Weather Maps Site. 04 June, 2002 .....	24
Figure 2.5 Computerized 500-mb Height Map (left) from the National Oceanic and Atmospheric Administration Central Library’s U.S. Daily Weather Maps Site. 14 June, 2012.....	25
Figure 3.1 Compared Frequencies of Chosen Onset Date Illustrated by Individual Parameter. Parameter Total is the sum of Temperature Criterion 1, Temperature Criterion 2 and 500-mb Heights. The frequency of choice is indicated along the x-axis, and the chronological onset date is located along the y-axis.. .....	35
Figure 3.2 Frequency of Onset Date Dictated by 500-mb Heights. The frequency of onset is indicated along the x-axis, and the chronological onset date is located along the y-axis... ..	46
Figure 3.3 Frequency of Onset Date Dictated by Temperature Criterion 1: The First Date of a Fifteen-Day Consecutive Period Where the Mean Temperature Exceeds 70.0°F (21.1°C), and at Least Ten of Those Fifteen Days Have a Temperature at, or Exceeding, 75.0°F (23.9°C). The frequency of onset is indicated along the x-axis, and the chronological onset date is located along the y-axis.....	52
Figure 3.4 Frequency of Onset Date Dictated by Temperature Criterion 2: The First Date of a Fifteen-Day Consecutive Period Where the Maximum Temperature Exceeds 77.0°F (25.0°C) and at Least Ten of Those Fifteen Days Have a Temperature at, or Exceeding, 82°F (27.8°C). The frequency of onset is indicated along the x-axis, and the chronological onset date is located along the y-axis.....	54
Figure 3.5 Frequency of Onset Date Dictated by 500-mb Heights as Compared to a Theoretically Normalized Distribution. The chronological date is binned into multiples of eight on the x-axis, and the frequency of the onset date is indicated on the y-axis.....	58
Figure 3.6 Frequency of Onset Date Dictated by Temperature Criterion 1 as Compared to a Theoretically Normalized Distribution. The chronological date is binned into multiples of eight on the x-axis, and the frequency of the onset date is indicated on the y-axis. ....	58
Figure 3.7 Frequency of Onset Date Dictated by Temperature Criterion 2 as Compared to a Theoretically Normalized Distribution. The chronological date is binned into multiples of eight on the x-axis, and the frequency of the onset date is indicated on the y-axis. ....	59

Figure 3.8 Frequency of Onset Date Dictated by a Summation of the Three Analyzed Parameters of 500-mb Heights, Temperature Criterion 1 and Temperature Criterion 2 as Compared to a Theoretically Normalized Distribution. The chronological date is binned into multiples of eight on the x-axis, and the frequency of the onset date is indicated on the y-axis. .... 59

Figure 3.9 Frequency of Final Chosen Onset Date as Compared to a Theoretically Normalized Distribution. The chronological date is binned into multiples of eight on the x-axis, and the frequency of the onset date is indicated on the y-axis. .... 60

**TABLE** **PAGE**

Table 1-1 Temperature and Precipitation Normals for Jefferson City, 1971-2000. Temperatures are in degrees Fahrenheit and precipitation is measured in inches ..... 3

Table 2-1 Jefferson City Station Timeline. Column 1 indicates years of importance, Column 2 outlines change of station conditions and Column 3 pertains to the application of data for this study. The Jefferson City Water Plant is: 38.35°N, 92.11°W, 670 feet in elevation, Station Index of 4271, Division 3 (West Central Plains), Cole County ..... 15

Table 2-2 Center for Ocean-Atmospheric Prediction Studies Japan Meteorological Agency El Niño Southern Oscillation Index, 1948 to present. Modes are El Niño (EL), La Niña (LA) and Neutral (NEU)..... 18

Table 2-3 Center for Ocean-Atmospheric Prediction Studies Pacific Decadal Oscillation Index, 1946 to present. Modes are high (positive) and low (negative)..... 19

Table 2-4 El Niño Southern Oscillation coupling with Pacific Decadal Oscillation in the Midwest, 1948-2013, as outlined by Birk et al. (2010). ENSO modes are El Niño (EL), La Niña (LA) and Neutral (NEU). PDO modes are high (POS) and low (NEG). Combined outcome shows two variables. Left: coupled temperature tendency: equal chances of warm/cool (Eq), warm (Wa) and cool (Co). Right: coupled precipitation tendency: equal chances wet/dry (Eq), wet (We) and dry (Dr). .... 20

Table 2-5 Standard Deviation Data for the Columbia Regional Airport (COU), Along with 30-Year June Average..... 26

Table 3-1 Results. Years of this study are indicated in the farthest left-hand column. The transition date chosen from the 500-mb geopotential height criterion is in the second column, with no data gathered between 1948-1967. The chosen date for the first temperature selection criterion is in the third column, with the date for the second criterion in the fourth column. The fifth column indicates the twenty-four-hour rainfall accumulation amount (in inches) for the significant rainfall event preceding the final chosen date, along with the number of dry days that elapsed between the rainfall event and the transition date (in parentheses). Bolded numbers in the fifth column show whether significant rainfall that occurred on the chosen transition day; if so, that amount is listed in inches. If rain occurred on the chosen transition day but it was not significant (i.e. it did not meet the 0.25-inch minimum threshold), it was not recorded. The sixth column illustrates the next significant twenty-four-hour rainfall accumulation event (in inches) after the final chosen date, along with the number of dry days that elapsed between the transition date and the rainfall event (in parentheses). The seventh column outlines the predicted coupling of ENSO/PDO, and what effect that should have on these temperatures and precipitation amounts. The eighth column indicates the final onset date chosen by this study..... 30

Table 3-2 Statistics of Onset Dates per Parameter, 1948-2013. Mean, median and mode of each parameter are listed by row, with each parameter listed by column. Final chosen date mean, median and mode can be found in the fourth column..... 34

Table 3-3 Frequency and Spread of Chosen Onset Dates within the Analyzed Months of May, June and July. The May, June and July rows indicate the number of times an onset date was chosen in that month. The spread row shows the number of whole days between earliest

chosen onset date and latest chosen onset date for an individual parameter. Each parameter is listed by column, with the final chosen date in the fourth column.....	34
Table 3-4 Frequency of Methodology Application for the Final Transition Date, 1968-2013. Average refers to a $\pm$ ten-day average of all three variables. Outlier refers to an average of two days within a ten-day range, excluding one outlier beyond the ten-day maximum threshold. Median refers to years with all data points greater than ten days apart, leading to the choice of the middle onset value.....	35
Table 3-5 The Statistics of the Nine Phases of ENSO, 1948-2013. The first row lists the number of years spent in each phase in this data set. The second and third rows illustrate the median and mode for each condition, respectively. The fifth row outlines the qualitative summer onset date expectation from Ratley et al. (2002). The phases are indicated by the starting phase in October of one year, and the phase designated by the next fall, using Neutral (NE), La Niña (LA) and El Niño (EL).....	39
Table 3-6 The Years of the Nine Phases of ENSO, 1948-2013. Phases are indicated by the starting phase in October of a year, and the phase designated by the next fall, using Neutral (NE), La Niña (LA) and El Niño (EL).....	41
Table 3-7 PDO Phases and Average Summer Onset Dates from this Study. Phases are indicated by -PDO (low) and +PDO (high) .....	42
Table 3-8 Statistics of Summer Onset Dates in ENSO Neutral Mode under PDO Phases. Phases are indicated by -PDO (low) and +PDO (high).. .....	43
Table 3-9 Statistics of Summer Onset Dates in ENSO La Niña Mode under PDO Phases. Phases are indicated by -PDO (low) and +PDO (high).. .....	43
Table 3-10 Statistics of Summer Onset Dates in ENSO El Niño Mode under PDO Phases. Phases are indicated by -PDO (low) and +PDO (high).. .....	43
Table 3-11 Coupled-Effect Expectations of ENSO/PDO on Rainfall in Missouri. Data indicate average number of whole dry days before and after final chosen summer onset for 1948-2013.....	45
Table 3-12 Contingency Table Comparing 500-mb Heights to Temperature Criterion 2. Independent y-axis compares 500-mb geopotential height onset dates to potentially dependent x-axis of Temperature Criterion 1 onset dates. Categorical columns are chosen to show a relationship if onset dates are within twenty-four hours of one another. Degrees of freedom, k, are calculated by (row – 1) multiplied by (column – 1).....	48
Table 3-13 Contingency Table Comparing 500-mb Heights to Temperature Criterion 2. Independent y-axis compares 500-mb geopotential height onset dates to potentially dependent x-axis of Temperature Criterion 2 onset dates. Categorical columns are chosen to show a relationship if onset dates are within twenty-four hours of one another. Degrees of freedom, k, are calculated by (row – 1) multiplied by (column – 1).....	49
Table 3-14 Differences in Chosen Final Onset Date Between this Research and Ratley et al. (2002) during 1981-2000. The fourth column illustrates number of whole days that elapsed between the chosen date of this research and the chosen date by Ratley et al. (2002). A zero (0) indicates that the chosen dates fell within twenty-four hours of one another. Numbers in the fourth column are qualified with a marker to show that this research chose the summer onset date earlier (E) or later (L) than Ratley et al. (2002).....	63

# AN ANALYSIS OF THE SPRING-TO-SUMMER TRANSITION IN THE WEST CENTRAL MISSOURI PLAINS

Rosalie Newberry

Dr. Anthony R. Lupo, Thesis Supervisor

## **ABSTRACT**

The spring-to-summer transition is of special importance in forecasting, as the general circulation undergoes an energy shift to a warmer regime, which affects the Midwestern United States. Beginning at the most localized scale, temperature variables are observed from surface observations at a representative station in the West Central Missouri Plains to identify the shift from late spring to early summer, with chosen guidelines for maximum temperature thresholds. Precipitation is analyzed as a summer onset validation tool, in the form of heavy precipitation event frequencies. From an upper-air analysis perspective, 500-mb height observations are examined to find a spring/summer transitional date from a chosen height minimum, as a surrogate for the jet stream, and thus a proxy for atmospheric kinetic energy. Finally, teleconnections on the planetary scale, specifically the influence of El Niño Southern Oscillation (ENSO) and Pacific Decadal Oscillation (PDO), are examined to aid in identifying the change of regime and its interannual variability. Isolating an approximate day or smaller time frame focus for the spring/summer transition will facilitate the ability to forecast seasonal pattern changes, as well as the seasonal potential for severe weather in the Missouri Plains. This, in turn, will provide safer, more economical outcomes for the population of this area.

# Chapter 1 INTRODUCTION

Missouri is a state that exhibits strong seasonality, from record high temperatures above 43°C (110°F) in the height of summer to record low temperatures colder than -28°C (-20°F) in the depths of winter (“Climatology and Weather Records,” [www.crh.noaa.gov](http://www.crh.noaa.gov)). The exact transition between the cold and warm seasons is often difficult to pinpoint, and can be highly valuable to a short-term forecaster, and even more so for a long-term one, as the transition signals a change of weather patterns that is more visible on an extended time scale. This work specifically aims to help detect the shift between spring and summer in the West Central Plains of the state of Missouri. Empirically, the spring-to-summer transition is a recognized problem in dynamic meteorology. Though seasonal shifts are common research phenomena (more than 9,000 articles appear in a basic “Seasonal shifts” search from the American Meteorological Society’s online journals, [www.journals.ametsoc.org](http://www.journals.ametsoc.org)), fewer than ten published academic research papers focus specifically on the spring-to-summer shift of Missouri (Ratley et al. 2002). It is important to extend knowledge for this area, so that long-range forecasters and future models can accurately and precisely predict seasonal changes, which will in turn impact different sectors of Missouri’s culture and economy.

The spring-to-summer change is both difficult to recognize and could be of special importance for what is colloquially known as the severe weather season in Missouri, where frequencies of severe thunderstorms and tornadoes are highest. Figure 1.1 shows the average number of tornadoes in the continental U.S. by month (“Historical Records and Trends,” [www.ncdc.noaa.gov](http://www.ncdc.noaa.gov)).

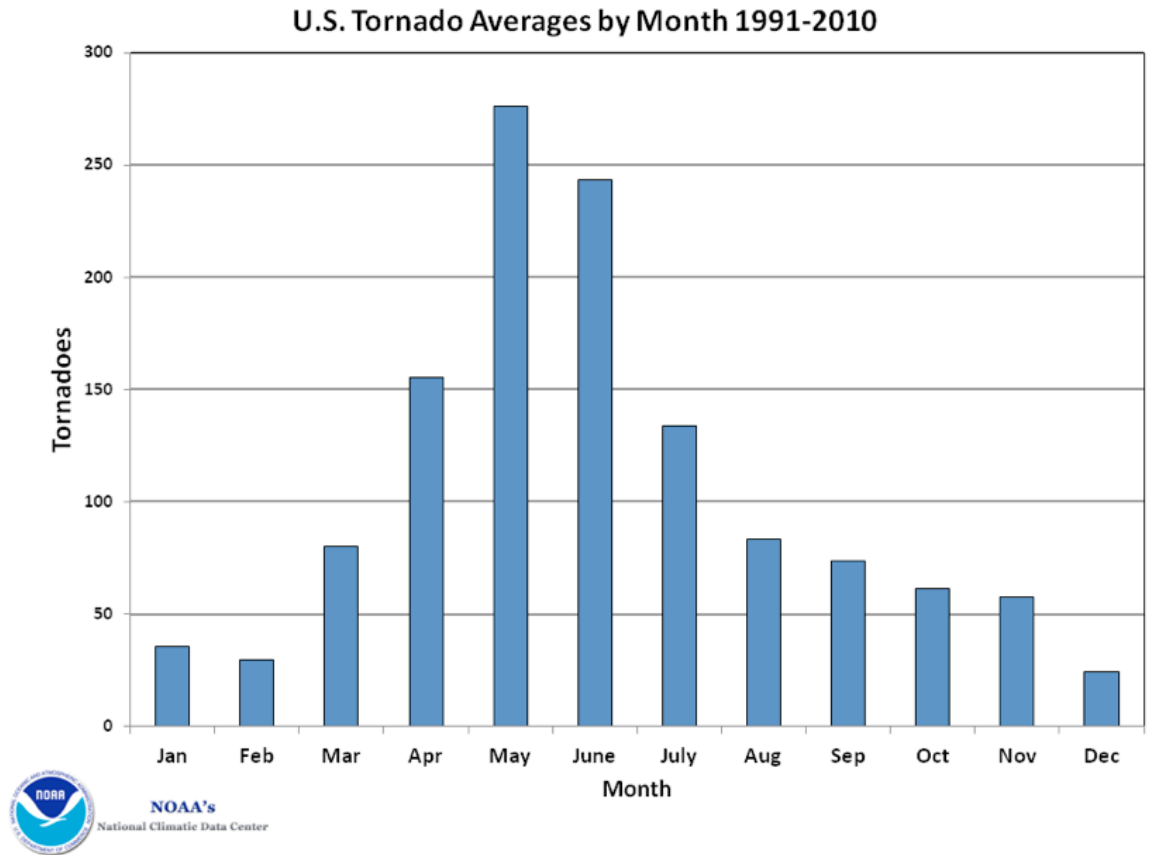


**Figure 1.1 U.S. Tornado Averages by Month from 1991-2010, published by the National Climatic Data Center, a Division of the National Oceanic and Atmospheric Administration.**

The spring season, March to May, produces a slightly greater number of tornadoes on average than the summer season, June to August, though the height of activity falls between May and June, when the two seasons are transitioning. The detection of the shift between spring and summer highlights not only a

decrease in the overall severe weather activity in Missouri, but also a change in daily temperature and precipitation patterns.

Spring is known to be a mild and frequently wet time for the state. Summer morphs into a period of high temperatures, high humidity and dry periods interjected with episodes of convective precipitation. Though three-month rain averages for March-April-May are less than half an inch different than averages for June-July-August, the precipitation normal for the state from 1971-2000 is actually greater during the summer set at a chosen representative site, in Jefferson City (as seen in Table 1-1, “Climatological Data Annual Summary 2012” [www.ncdc.noaa.gov](http://www.ncdc.noaa.gov)).

	MARCH	APRIL	MAY	JUNE	JULY	AUGUST
TEMPERATURE	6.56 °C (43.8 °F)	12.39 °C (54.3 °F)	17.61 °C (63.7 °F)	22.61 °C (72.7 °F)	25.5 °C (77.9 °F)	24.56 °C (76.2 °F)
PRECIPITATION	3.00”	4.14”	5.17”	4.39”	4.31”	4.04”

**Table 1-1 Temperature and Precipitation Normals for Jefferson City, 1971-2000. Temperatures are in degrees Fahrenheit and precipitation is measured in inches.**

Theoretically, this is due to heavy precipitation events, which have fewer occurrences than the stratiform systems of spring. Thus the frequency of precipitation events, especially those with significant rainfall, is of higher importance in the spring-to-summer transition than total rainfall amounts.

Logically, temperatures are expected to increase from the spring into the summer in the Midwest, and Missouri is no exception. The 30-year normal for Jefferson City (1971-2000) shows monthly average temperatures rising through the 40s, 50s and 60s in degrees Fahrenheit (five, ten and fifteen degrees Celsius) for the each of the spring months, respectively (“Climatological Data Annual Summary 2012” [www.ncdc.noaa.gov](http://www.ncdc.noaa.gov)). By comparison, each of the summer months boasts an average temperature above the 70-degree Fahrenheit mark (21-degree Celsius mark). The shift between spring and summer exhibits a change from the rockier temperature swings of spring to the steadier (and more predictable) warm temperatures of summer.

Forecasters often use upper-air data as the indicators of surface manifestations; the mandatory 500-mb level is a standard among these data (Ahrens, 2012). 500-mb geopotential height contours are a gauge for the amount of warmth in the middle levels of the atmosphere, as heights increase with rising temperatures. By examining a change in the 500-mb height field over an extended period of time, one can identify periods of warmer and cooler atmospheric conditions, but also periods of atmospheric excitation and relatively mean energy states, which are seasonal markers (Spar, 1949).

At the largest atmospheric scale, global patterns can be utilized to aid in forecasting, even down to a local level. Though normal gravity-inertia waves have a lifespan of seven to nine days, there are different varieties of planetary oscillations that can impact daily waves for months, years and even decades (Ahrens, 2012). Two important oscillations for the official classification of spring and summer in Missouri are ENSO, or El Niño Southern Oscillation, and PDO, or

Pacific Decadal Oscillation. The phases of these systems independent of one another alone would impact Missouri weather, but when certain phases of the two oscillations are combined, they have unique impacts on Missouri temperature and precipitation (Birk et al., 2010).

The observance of teleconnections, or the relation of climate anomalies at distances in the thousands of meters, was first noted by Sir Gilbert Walker in the early twentieth century (“Sir Gilbert Walker,” [www.walker-institute.ac.uk](http://www.walker-institute.ac.uk)). His foci were the same foci as this research: he calculated temperature and precipitation patterns that would be affected by pressure rises and falls in the genesis region of ENSO, the western Pacific. He was one of the first scientists to study such ENSO effects.

Since his groundbreaking work, scientists all over the world have examined temperature and precipitation outcomes with an ENSO parameter. Grimm and Tedeschi (2009) looked at significant rainfall patterns in South America during ENSO’s three modes, noting that ENSO phases changed rainfall with a quasi-symmetric pattern. Muñoz et al. (2010) argued for the expansion of the idea of ENSO teleconnections into the Intra-Americas Seas, i.e. the Gulf of Mexico and the Caribbean Sea, citing that ENSO patterns affect the two bodies of water in opposite ways. Many researchers have focused on the impact ENSO has on yearly monsoons, including Australian and Asian monsoons (Fasullo and Webster (2002) and Wu and Kirtman (2007) are some recent examples).

The most applicable studies to this research, though, examined ENSO effects in North America. Shinker and Bartlein (2009) utilized National Centers for Environmental Prediction/National Center for Atmospheric Research

(NCEP/NCAR) reanalysis data to demonstrate the connection between strong ENSO phases and upper-air data in North America, including 500-mb geopotential heights and 850-mb specific humidity. Mo (2010) defined a change in ENSO impacts, showing that the genesis of ENSO, whether it be in the eastern Pacific or central Pacific, changes the effects of the modes in North America.

This study is based on the ideas of researchers who coupled the North American ENSO effects with the impacts of PDO. Hu and Huang (2009) examined dry and wet conditions in the U.S. Great Plains, demonstrating that ENSO and PDO coupling can intensify ENSO phases. Birk et al. (2010) followed this idea, concentrating specifically on the Midwest to outline the regional effects of ENSO/PDO coupling.

## 1.1 – PURPOSE

The purpose of this study is based on the framework of the research published by Ratley et al (2002). The motivation for this work is to continue to provide new insight into the climatological transition of seasons in Missouri, specifically the change between the spring and summer seasons, as this transitional period makes current weather modeling and forecasting difficult. Planetary-scale oscillations are considered to have some influence, though they do not have direct impacts on the Midwest, and Missouri in particular (Ahrens, 2012). This paper will be the first to combine the potential impacts of multiple planetary-scale oscillations with localized data to help guide the forecasting of a summer onset.

The authors Ratley et al. (2002) chose Jefferson City as the representative site for the “East-Central Ozarks region of Missouri,” and selected five parameters to study the shift between the two seasons over a period of twenty years, from 1981-2000.

The five parameters examined will largely mirror the scope of this body of work, with a few changes. Ratley et al. (2002) investigated daily temperature and precipitation patterns for Jefferson City, using nine cooperative National Weather Service sites as quality control data to rule out measurement anomalies. This work will also use daily temperature and precipitation from Jefferson City, though the scope of the data coverage will be more focused and chronologically expanded.

Ratley et al. (2002) also utilized 500-mb heights in two ways. The first analysis of 500-mb data was to identify a minimum height requirement for the spring-to-summer transition date. The second was as a power surrogate for energy in the atmosphere: by identifying specific wave numbers and summing them over a period of 250 days, a bimodal pattern emerged, indicating periods of high and low kinetic energy in the 500-mb height field. This work will also analyze 500-mb data, but only in the former sense of these two options. This paper aims to focus this variable, too, on a smaller pinpointed timeframe compared to Ratley et al. (2002), but with a wider chronological scope.

Finally, Ratley et al. (2002) examined larger atmospheric scales to determine effects on Missouri climate patterns. ENSO was of particular interest to these authors, because the teleconnections created by the oscillation are largely familiar to Missouri; it is well-documented that changes in ENSO patterns affect

North American weather (Shinker and Bartlein, 2009; Hu and Huang, 2009 and Hu and Feng, 2012 are some recent examples). Though the periods of the modes are irregular, ENSO events last on average two to seven years, so the occurrence of ENSO phenomena in the U.S. is relatively frequent. This research will examine ENSO over a longer timeframe than Ratley et al. (2002), and will also include another pertinent oscillation, PDO, that has a tendency to interact with certain ENSO modes, changing the expected outcome of temperature and precipitation (Birk et al., 2010).

## 1.2 – OBJECTIVES

The rationale behind this work is to reexamine the previous study done by Ratley et al. (2002). The objectives are threefold:

1. To reevaluate the clarity of the scientific method used in collecting the original data set, which included the variables of daily temperature, precipitation, 500-mb height fields and ENSO effects from 1981-2000.
2. To strengthen any weak mathematical or logical arguments in the original work, even if that includes introducing or deleting certain variables.
3. To expand the chronological coverage of the appropriate variables both back in time and closer to the current date, yielding a more climatologically sound line of reasoning to lead to forecasting more precise and accurate summer start dates.

## **Chapter 2 DATA SELECTION METHODOLOGY**

### **2.1 – TIME SERIES SELECTION**

The work published by Ratley et al. (2002) examined spring-to-summer transitions for twenty years, from 1981-2000. The scope of this work aims to expand the same data set, both backward and forward in time. Climatology studies generally assume a period of thirty years, which makes the expansion of at least one decade important for this set of data (Ahrens, 2012).

The time period for research used here is 1948 to 2013, with the exception of 500-mb heights. These are used beginning in 1968, for ease of data acquisition, and since before this time upper-air analyses are assumed to be less reliable. For this study, only observational data were used. The National Centers for Environmental Prediction/National Center for Atmospheric Research Reanalysis Project ([www.esrl.noaa.gov/psd/data/reanalysis](http://www.esrl.noaa.gov/psd/data/reanalysis)) is a netCDF-based service that displays assimilated data from 1948 to the present. It provided the basis for the choice of lower temporal bound for this work. The upper bound was chosen due to available data: at the time of writing, spring and summer had both concluded for 2013. Thus the inclusive set of this work spans sixty-six years.

The work by Ratley et al. (2002) identified twenty summer transition dates. The mean, median and mode all fell in June; only one May date was

selected (21 May, 1991) and only one July date was selected (01 July, 2000).

Though Ratley et al. (2002) examined temperatures and precipitation from April to September, this work focuses more sharply on the best candidates for a summer start date: May, June and July.

To filter out synoptic-scale data, the thresholds for temperature, precipitation and 500-mb heights are set on a ten- to fifteen-day scale. A typical synoptic-scale wave lasts from one to seven days (Ahrens, 2012). Additionally, the largest- (planetary-) scale weather patterns (e.g. temperature, pressure and winds) have a well-known ten- to fourteen-day oscillation period, which is roughly the limit of dynamic predictability (Lorenz 1963, 1969). This vacillation is the natural period that derives from the scale analysis of solutions to the equations of motion, these being dependent on the size and rotation rate of the planet. By filtering out synoptic-scale anomalies, large-scale data are captured (Ratley et al., 2002).

## 2.2 – LOCATION SELECTION

The authors Ratley et al. (2002) chose Jefferson City, Missouri as the principal site of data collection in their work, and as the representative site of the entire East-Central Missouri Ozarks. They used a mixture of geographical and anthropogenic borders to outline the area of focus, which can be seen in Figure 2.1. These borders loosely include the western edge of the East Ozarks, the Mississippi River to the east, the Missouri River to the north and the Missouri/Arkansas border to the south. Or, more broadly, the territory involved was the southeastern quadrant of the state, with the Bootheel being excluded.

Utilizing the idea of principal component analysis set forth by Palecki and Leathers (2000), Ratley et al. (2002) showed that focusing on Jefferson City's data is sufficient to make conclusions about the East-Central Missouri Ozarks region as a whole. The results of Palecki and Leathers (2000) suggested that Jefferson City would represent a larger area than chosen for the Ratley et al. (2002) study.

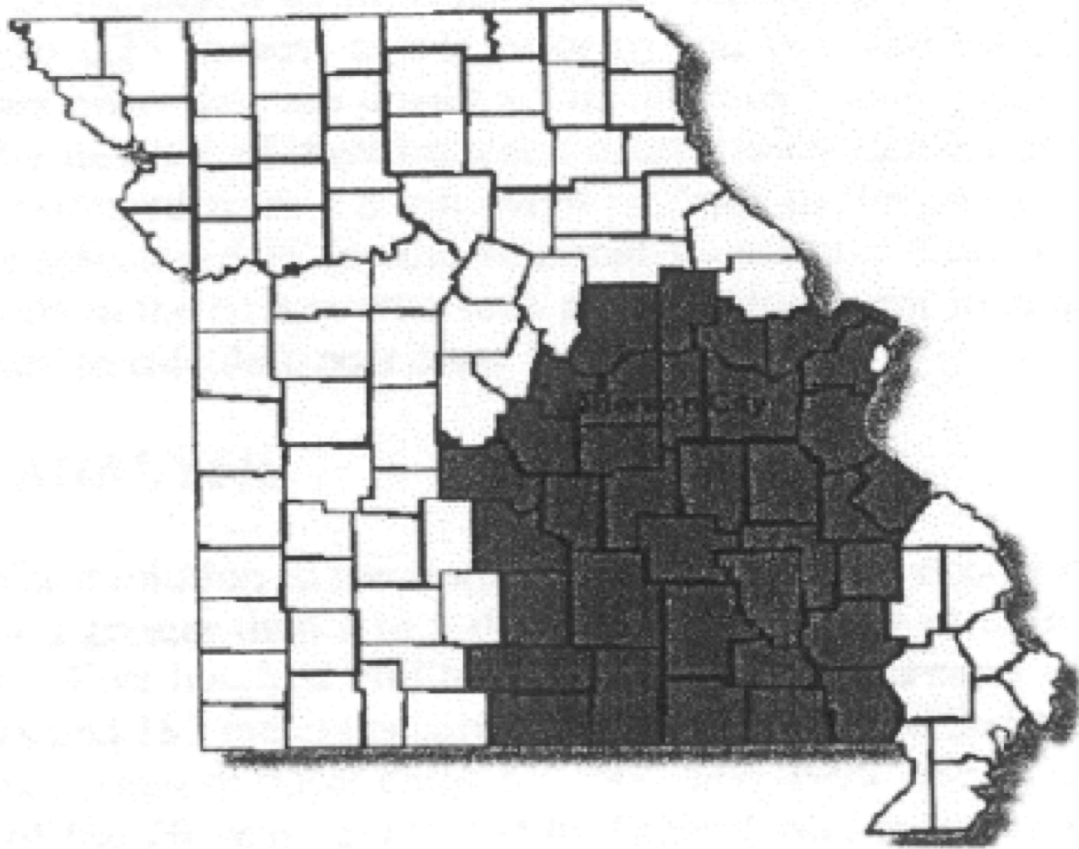


**Figure 2.1 Ratley et al. (2002) Location Selection, including Jefferson City, Missouri, 1981-2000. This area is bounded by the edge of the East Ozarks to the west, the Mississippi River to the east, the Missouri River to the north and the Missouri/Arkansas border to the south.**

This work also uses Jefferson City as its principal and representative data site, but for a different region. In 1948, Jefferson City was located in the

Southwestern Division of the U.S. Department of Commerce Weather Bureau's "Climatological Data: Missouri Section," which is where official reports for the state's weather patterns can be found, that date as far back as 1884 ("Climatological Data Publications," [www.ncdc.noaa.gov](http://www.ncdc.noaa.gov)). By 1957, however, the same publication reorganized its previous three-section model (which included Northern, Southwestern and Southeastern divisions) into a six-section model. The divisions came to include Northwest Prairie, Northeast Prairie, West Central Plains, West Ozarks, East Ozarks and the Bootheel, and it is still the divisional system in use today. Figure 3 outlines these divisions, with Jefferson City in the West Central Plains.

It's important to recognize that the U.S. Department of Commerce Weather Bureau reorganized these divisions so that data would be categorized into subgroups with "similar climatological characteristics" (Reference Notes, "Climatological Data: Missouri," 2013. [www.ncdc.noaa.gov](http://www.ncdc.noaa.gov)). This is noteworthy, because it changes the outlook for data application from the work by Ratley et al. (2002). Figure 2.2 illustrates that the 1957 reorganization set Jefferson City on the cusp of not just two, but three reporting divisions: Northeast Prairie, West Central Plains and East Ozarks.



**Figure 2.2 United States Department of Commerce Weather Bureau’s “Climatological Data: Missouri Section,” Divisions, 1957 to Present.**

Since Ratley et al. (2002) were able to use principal component analysis by Palecki and Leathers (2000) to apply Jefferson City data to the East Central Missouri Ozarks region as a whole, the same logic leads to the validity of using Jefferson City as the representative site for all three aforementioned divisions. In fact, Jefferson City is the farthest from the East Ozarks mentioned by Ratley et al. (2002), roughly twenty to thirty miles, but it is less than ten miles away from the beginning of the Northeast Prairie, where sister site Columbia is located. For site continuity during this project, Jefferson City is used, though standard deviations for monthly temperature and precipitation averages from Columbia are

applicable. There must be recognition of the extent of this application, as there is a valid radius of use within the state. Columbia falls within this radius, due to climatological similarities and geographical location relative to Jefferson City. This research assumes such climatic similarity from the chosen station location to the rest of its reporting division. Huff and Changnon (1986) demonstrated that precipitation anomalies due to the urbanization of St. Louis, Missouri are negligible throughout the course of a year. The same principle applies to the Urban Heat Island effect, which was shown by Peterson (2003) to have no significant outcome on temperatures in a rural situation versus an urban one. Thus Jefferson City will be an unbiased urban choice for this research.

Jefferson City's reporting site moved three times during the course of the years of this study, 1948-2013, meaning there were four reporting sites used in total. This number is one more than the proposed necessary number for minimum site change as set forth by Birk et al. (2010). However, every Jefferson City site falls easily within one degree of longitude and latitude of the other, and one site reported for just one year (1948) so this discrepancy is ignored. Only one site option was given in 1948, but starting as early as 1949, the KWOS Radio Station began reporting in Jefferson City as well, giving a second data collection option. Between the two sites, KWOS was the only station in subsequent years that reported both temperature and precipitation, as the original site stopped reporting temperatures. In 1950, Lincoln University began reporting temperatures and precipitation as well. This site was ignored until 1957, when it became the only continuously-reporting station for the area. In 1977, the Jefferson City Water Plant began reporting daily temperatures and precipitation,

and it remained the primary data site until the end of the period covered by this research, 2013. Table 2-1 illustrates the timing of stations reporting in Jefferson City, and the changes of station choice.

1884	State meteorological records begin	
1890	Jefferson City records begin; J. C. Halligan, Observer.	(1948: the research for this paper begins.)
1949	A second station begins reporting; newest is KWOS Radio.	(1949 on: KWOS Radio is the station used in this work.)
1950	A third station begins reporting; newest is Lincoln University.	(1957 on: Lincoln University is the station used in this work.)
1964	State divisions are reorganized, putting Jefferson City in the West Central Plains.	
1977	A new station begins reporting; newest is the Jefferson City Water Plant.	(1977 on: the Water Plant is the station used in this work.)
2013	Jefferson City Water Plant continues to report for daily records.	(2013: the research for this paper concludes.)

**Table 2-1 Jefferson City Station Timeline. Column 1 indicates years of importance, Column 2 outlines change of station conditions and Column 3 pertains to the application of data for this study. The Jefferson City Water Plant is: 38.35°N, 92.11°W, 670 feet in elevation, Station Index of 4271, Division 3 (West Central Plains), Cole County.**

The Jefferson City Water Plant is the station with the most longevity, and it encompasses the bulk of data collected in this research. The Jefferson City Water Plant has the following characteristics: 38.35°N, 92.11°W, 670 feet in

elevation, Station Index of 4271, Division 3 (West Central Plains), Cole County. As dictated by the National Climatic Data Center, temperature is noted at its maximum, regardless of time of day. Precipitation is recorded to hundredths of an inch in liquid water equivalent totals (Reference Notes, “Climatological Data: Missouri,” 2013. [www.ncdc.noaa.gov](http://www.ncdc.noaa.gov)).

## 2.3 – DATA SELECTION

### 2.3.1 – OSCILLATION SELECTION

El Niño Southern Oscillation (ENSO) and Pacific Decadal Oscillation (PDO) are the two main planetary influences considered in this research. The support for the decision to use these two oscillations as interconnected cycles stems from the published research by Birk et al. (2010).

The Japan Meteorological Agency has published ENSO modes from 1868 to present (“JMA SST ENSO Index” [www.coaps.fsu.edu/jma](http://www.coaps.fsu.edu/jma)). The JMA’s SST (Sea Surface Temperature) ENSO Index and the area it encompasses have been widely used by other scholarly articles (Bove et al., 1998; Pielke and Landsea, 1999 and Huang et al., 2012 are some recent examples). Hanley et al. (2003) found that, while the JMA index is more sensitive to La Niña events than other modes, it is less sensitive than other indices to El Niño events. While it is imperfect, the JMA SST-based index approach is still a viable one, as other working indices have the same issue: sensitivity in one mode (including Niño-3.4, Niño-1+2 and Niño 3) (Hanley et al., 2003). The JMA classifies ENSO phases as follows:

1. El Niño: the SST anomaly must be  $0.5^{\circ}\text{C}$  or greater for six months consecutively, including October, November and December of a given year.
2. La Niña: the SST anomaly must be  $-0.5^{\circ}\text{C}$  or less for six months consecutively, including October, November and December of a given year.
3. Neutral: the SST anomaly must lie between  $-0.5^{\circ}\text{C}$  and  $0.5^{\circ}\text{C}$  for six months consecutively, including October, November and December of a given year.

These anomalies apply to a bounded region of  $4^{\circ}\text{S}$  to  $4^{\circ}\text{N}$ ,  $150^{\circ}\text{W}$  to  $90^{\circ}\text{W}$ . The JMA defines the inception of an ENSO year as 01 October, with its conclusion on 30 September of the next year (e.g. the El Niño year of 1969 began on 01 October, 1969 and ended on 30 September, 1970). Table 2-2 displays the JMA SST ENSO Index data from 1948 to 2013.

Year	Classification	Year	Classification	Year	Classification
1948	NEU	1970	LA	1992	NEU
1949	LA	1971	LA	1993	NEU
1950	NEU	1972	EL	1994	NEU
1951	EL	1973	LA	1995	NEU
1952	NEU	1974	LA	1996	NEU
1953	NEU	1975	LA	1997	EL
1954	LA	1976	EL	1998	LA
1955	LA	1977	NEU	1999	LA
1956	LA	1978	NEU	2000	NEU
1957	EL	1979	NEU	2001	NEU
1958	NEU	1980	NEU	2002	EL
1959	NEU	1981	NEU	2003	NEU
1960	NEU	1982	EL	2004	NEU
1961	NEU	1983	NEU	2005	NEU
1962	NEU	1984	NEU	2006	EL
1963	EL	1985	NEU	2007	LA
1964	LA	1986	EL	2008	NEU
1965	EL	1987	EL	2009	EL
1966	NEU	1988	LA	2010	LA
1967	LA	1989	NEU	2011	NEU
1968	NEU	1990	NEU	2012	NEU
1969	EL	1991	EL	2013	NEU

**Table 2-2 Center for Ocean-Atmospheric Prediction Studies Japan Meteorological Agency El Niño Southern Oscillation Index, 1948 to present. Modes are El Niño (EL), La Niña (LA) and Neutral (NEU).**

Pacific Decadal Oscillation positive and negative modes are catalogued by the Center for Ocean-Atmospheric Prediction Studies (COAPS), the same entity that logs ENSO modes ([www.coaps.fsu.edu](http://www.coaps.fsu.edu)). The most important effect of PDO is how it interacts with ENSO during certain phases to create an enhanced effect on temperatures and precipitation (Birk et al., 2010). The characteristics of these modes are less pronounced than those for ENSO due to PDO's fifty- to seventy-year cycle (as discussed by Mantua et al., 1997 and Minobe, 1997). COAPS registers PDO phases as follows:

1. High (+) PDO: cold SSTs in the north central and western Pacific Ocean, warm SSTs off the western coast of North America, with a deep Aleutian low.
2. Low (-) PDO: warm SSTs in the north central and western Pacific Ocean, cool SSTs off the western coast of North America, with no pronounced Aleutian low.

PDO warming and cooling is confined to the Pacific Ocean, at or above 20°N. Meteorological entities and agencies utilize climatologically average SSTs to determine high and low PDO phases (Ahrens, 2012). Table 2-3 illustrates the PDO high and low modes (positive and negative, respectively) from 1910 to present. Table 2-4 displays the coupling of ENSO and PDO as demonstrated by Birk et al. (2010).

Year Range	Mode
1910 – 1924	-PDO
1925 – 1946	+PDO
1947 – 1976	-PDO
1977 – 1998	+PDO
1999 - 2013	-PDO

**Table 2-3 Center for Ocean-Atmospheric Prediction Studies Pacific Decadal Oscillation Index, 1946 to present. Modes are high (positive) and low (negative).**

Year	ENSO Phase	PDO Phase	Combined Outcome
2013	NEU	NEG	EqDr
2012	NEU	NEG	EqDr
2011	NEU	NEG	EqDr
2010	LA	NEG	EqDr
2009	EL	NEG	EqEq
2008	NEU	NEG	EqDr
2007	LA	NEG	EqDr
2006	EL	NEG	EqEq
2005	NEU	NEG	EqDr
2004	NEU	NEG	EqDr
2003	NEU	NEG	EqDr
2002	EL	NEG	EqEq
2001	NEU	NEG	EqDr
2000	NEU	NEG	EqDr
1999	LA	NEG	EqDr
1998	LA	POS	EqWe
1997	EL	POS	WaDr
1996	NEU	POS	EqWe
1995	NEU	POS	EqWe
1994	NEU	POS	EqWe
1993	NEU	POS	EqWe
1992	NEU	POS	EqWe
1991	EL	POS	WaDr
1990	NEU	POS	EqWe
1989	NEU	POS	EqWe
1988	LA	POS	EqWe
1987	EL	POS	WaDr
1986	EL	POS	WaDr
1985	NEU	POS	EqWe
1984	NEU	POS	EqWe
1983	NEU	POS	EqWe
1982	EL	POS	WaDr
1981	NEU	POS	EqWe
1980	NEU	POS	EqWe
1979	NEU	POS	EqWe
1978	NEU	POS	EqWe
1977	NEU	POS	EqWe
1976	EL	NEG	EqEq
1975	LA	NEG	EqDr
1974	LA	NEG	EqDr
1973	LA	NEG	EqDr
1972	EL	NEG	EqEq

1971	LA	NEG	EqDr
1970	LA	NEG	EqDr
1969	EL	NEG	EqDr
1968	NEU	NEG	EqDr
1967	LA	NEG	EqDr
1966	NEU	NEG	EqDr
1965	EL	NEG	EqEq
1964	LA	NEG	EqDr
1963	EL	NEG	EqEq
1962	NEU	NEG	EqDr
1961	NEU	NEG	EqDr
1960	NEU	NEG	EqDr
1959	NEU	NEG	EqDr
1958	NEU	NEG	EqDr
1957	EL	NEG	EqEq
1956	LA	NEG	EqDr
1955	LA	NEG	EqDr
1954	LA	NEG	EqDr
1953	NEU	NEG	EqDr
1952	NEU	NEG	EqDr
1951	EL	NEG	EqEq
1950	NEU	NEG	EqDr
1949	LA	NEG	EqDr
1948	NEU	NEG	EqDr

**Table 2-4 El Niño Southern Oscillation coupling with Pacific Decadal Oscillation in the Midwest, 1948-2013, as outlined by Birk et al. (2010). ENSO modes are El Niño (EL), La Niña (LA) and Neutral (NEU). PDO modes are high (POS) and low (NEG). Combined outcome shows two variables. Left: coupled temperature tendency: equal chances of warm/cool (Eq), warm (Wa) and cool (Co). Right: coupled precipitation tendency: equal chances wet/dry (Eq), wet (We) and dry (Dr).**

### 2.3.2 – UPPER-AIR MAP SELECTION

Following the foundation laid by Ratley et al. (2002), 500-mb heights are the upper-air synoptic focus of this research. The criterion set forth by Ratley et al. (2002) for identifying the transition date for the beginning of summer is as follows:

The first date of a period persisting for at least 10 consecutive days where 500-mb heights are in excess of 5,820 m.

5,280 m is a geopotential height cutoff (in meters) that is indicative of the difference between the baroclinicity of the mid-latitudes and the quasi-barotropic nature of the subtropics (Ratley et al., 2002). This height minimum is the trailing equatorward edge of tightly-packed mid-latitude height gradients, as demonstrated in a derecho study by Bentley and Mote (1998), and in study of summer atmospheric perturbations by Wang et al. (2009). Due to its presence and persistence as the mean of height contours by June, it is chosen as the height requirement for this study (Ratley et al., 2002).

In this experiment, 500-mb height maps from 2003-2013 were made available by the National Oceanic and Atmospheric Administration (NOAA) Central Library's U.S. Daily Weather Maps site ([www.lib.noaa.gov](http://www.lib.noaa.gov)). For maps from 1968-2002, the site provided downloadable mailers, featuring daily weather maps sent in a weekly periodical. From 1984-2013, all maps were recorded in geopotential meters, but from 1968, the start of this research, to 1983, all 500-mb heights were reported in feet. In order to find the contour comparable to 5,820 meters, a conversion was made:

$$(5,820 \text{ meters})(3.28 \text{ feet/meter}) = 19,095 \text{ feet (rounded)}.$$

Due to the fact that height contours at that level are reported in intervals of 200 feet, the 19,100-ft line was sought, with the same 10-day consecutive requirement. 500-mb maps include height contours above sea level and isotherms calculated at 7:00 AM EST for the given day. The evolution of the 500-

mb maps from 1968 to 2002 is depicted in Figures 2.3 and 2.4. The introduction of the computerized 500-mb map is depicted in Figure 2.5.

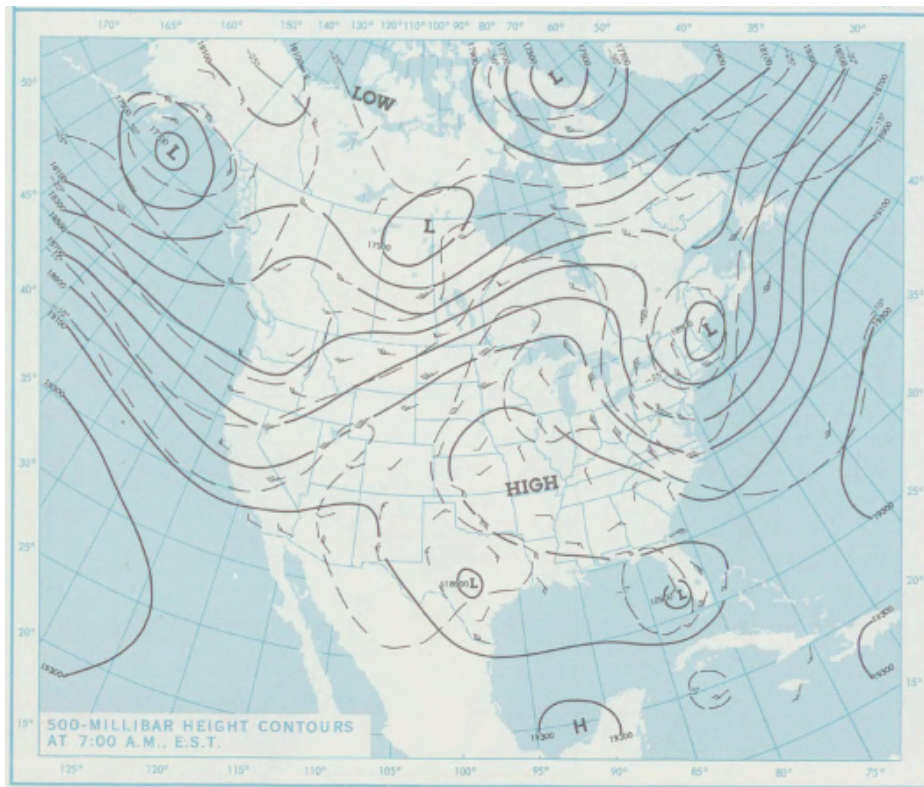


**Figure 2.3 500-mb Height Map from the National Oceanic and Atmospheric Administration Central Library's United States Daily Weather Maps Site. 19 June, 1968.**

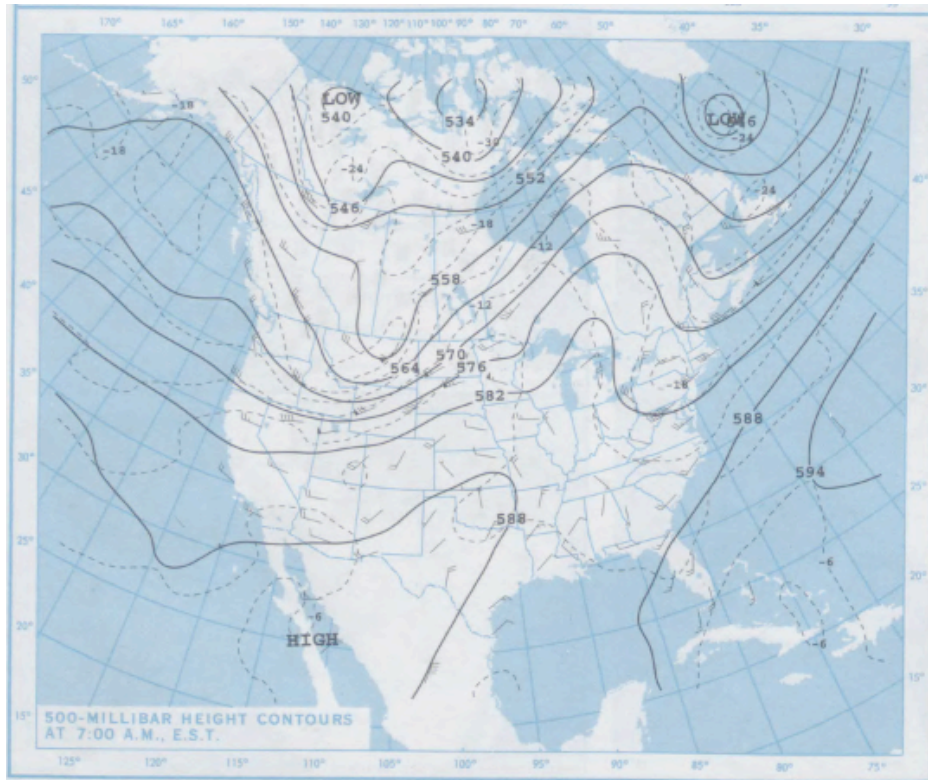


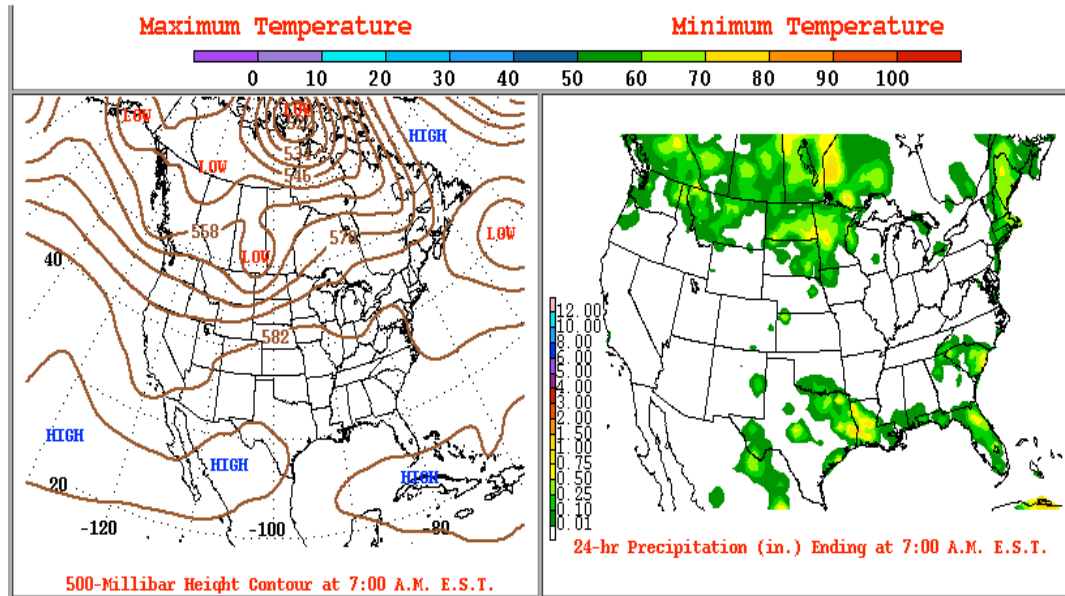
**Figure 2.4 500-mb Height Map from the National Oceanic and Atmospheric Administration Central Library's United States Daily Weather Maps Site. 04 June, 2002.**

# Daily Weather Maps

[PREVIOUS DAY](#)

THURSDAY JUNE 14, 2012

[NEXT DAY](#)



Prepared by the National Centers for Environmental Prediction, Hydrometeorological Prediction Center

**Figure 2.5 Computerized 500-mb Height Map (left) from the National Oceanic and Atmospheric Administration Central Library's U.S. Daily Weather Maps Site. 14 June, 2012.**

## 2.3.3 – STATISTICAL DATA SELECTION

Hart and Grumm (2001) among others showed that temperature and precipitation anomalies in the mid-latitudes tend to have a normal distribution. Hart and Grumm (2001) were able to rank synoptic-scale events from reanalysis data beginning in 1948. Synoptic-scale anomalies, which include daily temperature and precipitation, display a rarity of occurrence in direct correlation with the number of standard deviations from climatology normals in North America. Following the application of principal component analysis by Palecki and Leathers (2000), Ratley et al. (2002) chose the temperature threshold for the

spring-to-summer transition as one standard deviation below the monthly June mean. As a rule for normal distributions, one standard deviation above or below a mean should encompass about 68.27% of the total values of the data set. This was done to encourage a summer start date even if the overall summer was a cool one (Ratley et al., 2002).

Applying this same methodology, this work utilizes the 30-year average, 30-year standard deviation and 125-year standard deviation from Jefferson City’s neighboring site, Columbia Regional Airport, for the Jefferson City data. Table 2-5 outlines these data, along with the 125-year June mean, which stems back to 1889 (produced by National Climatic Data Center, [www.ncdc.noaa.gov](http://www.ncdc.noaa.gov)).

	30-YEAR AVERAGE (1971-2000)	30-YEAR STANDARD DEVIATION (1971-2000)	125-YEAR STANDARD DEVIATION (1884-2013)
NUMERICAL VALUE	22.72°C (72.90°F)	2.54°C (2.28°F)	3.26°C (2.93°F)

**Table 2-5 Standard Deviation Data for the Columbia Regional Airport (COU), Along with 30-Year June Average.**

The method for examining precipitation applies only one type of statistical analysis: frequency of dates between significant rainfall events (Ratley et al., 2002). The focus turns to significant precipitation based on a certain minimum, and the duration of dry periods between that type of event. As both spring and summer are expected to have convective events, the frequency between significant rainfall events is the indicator that a seasonal change has occurred. Carleton et al. (2008) discuss the convective nature of summers in the Midwest,

as atmospheric energy becomes more conducive to convective precipitation. Between such events, summer should have more prolonged dry periods (Ratley et al., 2002).

#### 2.3.4 – TEMPERATURE SELECTION

The criteria for a summer start date utilizing temperature as the focal variable are as follows:

1. The first date of a fifteen-day consecutive period where the mean temperature exceeds 70.0°F (21.1°C), and at least ten of those fifteen days have a temperature at, or exceeding, 75.0°F (23.9°C).
2. The first date of a fifteen-day consecutive period where the maximum temperature exceeds 77.0°F (25.0°C) and at least ten of those fifteen days have a temperature at, or exceeding, 82°F (27.8°C).

These thresholds follow the work by Ratley et al. (2002). Temperatures are selected in degrees Fahrenheit for ease of data acquisition, as the United States still largely reports observational data in U.S. customary units, not metric ones. A degree of correlation is expected to be present between the two temperature criteria, as both have to utilize a daily maximum temperature, but the effectiveness and usefulness of each parameter will be evaluated separately. This may guide future study, if an analysis of both variables is extraneous.

#### 2.3.5 – PRECIPITATION SELECTION

Precipitation is used as a validation parameter in this study. The selection of precipitation data should strengthen the argument for a specific choice of

summer onset date, as precipitation amounts in both spring and summer are highly influenced by more than one source. The criterion for confirming a summer start date using precipitation frequency as a parameter is as follows:

The number of days between significant rainfall events (greater than, or equal to, 0.25 inches). This threshold also follows the work by Ratley et al. (2002) for consensus.

### 2.3.6 – DATA ACCOUNTABILITY

The aim of this study is to have consensus between all three transition parameters of 500-mb geopotential heights, mean daily temperature and maximum daily temperature, with ENSO/PDO influences and precipitation frequency as validation parameters. Barring perfect consensus of a single chosen transition day, the following methodology is applied to select a final transition date:

1. Dates that are within ten days of one another are averaged, using a numerical assignment for each day in May, June and July: seventy-one days in total. Dates could be spread as far as twenty days apart for this method, but one date could be no more than ten days away from the next closest date. This follows the approach of synoptic-scale data.
2. If one date is the single outlier (i.e. greater than ten days) away from two dates that were within ten days of each other, the outlier is excluded.

3. If all dates are more than ten days apart, the middle date is selected for the final transition date. This is implemented so that high and low outliers will not overwhelm averages.

In each of these methods, a decimal average is rounded. If the value is less than 0.5, the date is rounded down, which follows basic mathematical reasoning. If the value is 0.5 or greater, the date is rounded up. Though this method may introduce error by straying from the original integer computed, it follows mathematical logic and, at most, would only change an onset date by twenty-four hours.

If Jefferson City did not report data for an entire month (due assumedly to a station malfunction), the lack of data is indicated with an asterisk (\*). Partial data, however, are used wherever applicable. If the year in question has no daily temperature/precipitation data and falls between 1948-1967, no summer transition date is chosen (i.e. no data is collected to lead to the choice of such a date). If the year in question has no daily temperature/precipitation data and falls between 1968-2013, 500-mb map data are the guidance for the summer transition date. If only one figure is missing from an otherwise complete data set (i.e. no temperature is reported on 04 July, but temperatures are reported on 03 July and 05 July), the two numbers from the surrounding days are averaged to fill the gap.

Any years with an “End of data” indicator show will show that no significant precipitation events have occurred before the data set ran out. In this instance, the number of whole dry (or insignificant rain) days that have already elapsed will become the numerical value for that quantity.

## Chapter 3 RESULTS AND ANALYSIS

### 3.1 — STUDY RESULTS

The results of the study are shown immediately below in Table 3-1.

Year	500-mb Height	Temperature Criterion 1	Temperature Criterion 2	Significant Precipitation: Before	Significant Precipitation: After	ENSO/PDO Expectation	FINAL DATE CHOSEN
2013	19-Jun	21-Jun	09-Jun	3.20 (12)	0.30 (0)	EqDr	16-Jun
2012	07-Jun	28-May	03-Jun	0.46 (22)	0.36 (6)	EqDr	02-Jun
2011	29-May	05-Jun	15-Jun	<b>0.45</b> 0.29 (0)	0.56 (18)	EqDr	06-Jun
2010	05-Jun	02-Jun	23-May	<b>0.32</b> 0.72 (0)	0.43 (11)	EqDr	31-May
2009	14-Jun	19-Jun	11-Jun	0.63 (1)	2.14 (2)	EqEq	15-Jun
2008	01-Jul	06-Jun	15-Jun	0.63 (0)	0.69 (0)	EqDr	11-Jun
2007	09-Jun	04-Jun	10-Jun	0.27 (9)	1.61 (1)	EqDr	08-Jun
2006	29-Jun	29-May	19-May	End of data (>15 days)	1.41 (13)	EqEq	24-May
2005	19-Jun	08-Jun	29-May	1.12 (6)	0.44 (10)	EqDr	03-Jun
2004	07-Jun	10-Jun	29-Jun	0.29 (9)	0.34 (1)	EqDr	28-Jun
2003	29-Jun	20-Jun	28-Jun	2.65 (2)	1.22 (10)	EqDr	26-Jun
2002	19-Jun	06-Jun	16-Jun	0.64 (4)	0.59 (14)	EqEq	14-Jun
2001	05-Jun	15-Jun	06-Jun	<b>1.95</b> 2.27 (4)	1.32 (1)	EqDr	09-Jun
2000	17-Jun	02-Jun	02-Jul	<b>1.22</b> 0.30 (4)	1.15 (3)	EqDr	10-Jun
1999	03-Jun	08-Jun	29-May	0.27 (13)	0.25 (0)	EqDr	03-Jun
1998	17-Jun	21-May	12-May	<b>0.40</b>	0.44 (11)	EqWe	23-May

				0.78 (1)			
1997	19-Jun	20-Jun	15-Jun	0.33 (0)	1.96 (4)	WaDr	18-Jun
1996	20-Jun	19-Jun	26-Jun	0.29 (11)	0.49 (0)	EqWe	22-Jun
1995	06-Jul	16-Jun	14-Jun	0.32 (5)	0.45 (11)	EqWe	15-Jun
1994	13-Jun	12-Jun	11-Jun	0.40 (2)	0.34 (10)	EqWe	12-Jun
1993	11-Jun	17-Jun	08-Jun	<b>2.33</b> 0.57 (2)	0.26 (11)	EqWe	12-Jun
1992	01-Jul	18-Jun	23-Jun	1.27 (19)	0.95 (5)	EqWe	24-Jun
1991	06-Jun	22-May	21-Jun	0.70 (6)	0.94 (9)	WaDr	22-May
1990	05-Jun	14-Jun	16-Jun	2.02 (4)	1.20 (6)	EqWe	12-Jun
1989	19-Jun	25-Jun	17-Jun	<b>0.94</b> 0.89 (4)	End of data (>22 days)	EqWe	20-Jun
1988	10-Jun	11-Jun	06-Jun	1.40 (15)	0.53 (21)	EqWe	09-Jun
1987	05-Jun	08-Jun	08-May	0.63 (0)	0.39 (12)	WaDr	07-Jun
1986	13-Jun	08-Jun	04-Jun	0.64 (13)	0.32 (18)	WaDr	08-Jun
1985	07-Jul	*	*	0.61 (15)	End of data (>3 days)	EqWe	07-Jul
1984	08-Jun	12-Jun	31-May	0.45 (7)	0.34 (0)	EqWe	07-Jun
1983	30-Jun	21-Jun	15-Jun	0.90 (0)	2.44 (2)	EqWe	22-Jun
1982	29-Jun	29-Jun	20-Jun	0.47 (6)	0.67 (0)	WaDr	26-Jun
1981	17-Jun	09-Jun	18-Jun	0.75 (1)	0.28 (0)	EqWe	15-Jun
1980	11-Jun	02-Jun	25-May	0.33 (3)	0.35 (8)	EqWe	02-Jun
1979	14-Jun	12-Jun	12-Jun	0.33 (2)	0.29 (6)	EqWe	13-Jun
1978	10-Jun	17-Jun	24-Jun	0.46 (11)	0.30 (7)	EqWe	17-Jun
1977	10-Jun	26-May	13-May	1.01 (5)	0.38 (3)	EqWe	26-May
1976	06-Jun	*	*	*	*	EqEq	06-Jun
1975	18-Jun	*	*	*	*	EqDr	18-Jun
1974	30-Jun	*	*	*	*	EqDr	30-Jun

1973	08-Jun	13-Jun	01-Jun	<b>0.97</b> 0.55 (0)	1.76 (9)	EqDr	07-Jun
1972	30-Jun	09-Jun	16-May	0.55 (2)	0.54 (7)	EqEq	09-Jun
1971	17-Jun	17-Jun	30-May	0.82 (5)	0.28 (10)	EqDr	17-Jun
1970	13-Jun	*	*	*	*	EqDr	13-Jun
1969	21-Jun	26-Jun	15-Jun	<b>3.27</b> 0.97 (3)	0.60 (0)	EqDr	21-Jun
1968	03-Jun	10-Jun	01-Jun	0.46 (1)	2.15 (22)	EqDr	05-Jun
1967	N/A	*	*	*	*	EqDr	*
1966	N/A	*	*	*	*	EqDr	*
1965	N/A	26-Jun	30-May	0.47 (6)	1.04 (1)	EqEq	13-Jun
1964	N/A	10-Jun	16-Jun	End of data (>8 days)	0.41 (14)	EqDr	13-Jun
1963	N/A	*	*	*	*	EqEq	*
1962	N/A	12-Jun	10-May	End of data (> 5 days)	0.96 (18)	EqDr	27-May
1961	N/A	18-Jun	28-May	0.32 (1)	0.25 (0)	EqDr	08-Jun
1960	N/A	17-May	14-May	0.83 (4)	1.22 (7)	EqDr	16-May
1959	N/A	03-Jul	03-Jun	<b>0.43</b> 1.47 (0)	0.44 (6)	EqDr	18-Jun
1958	N/A	13-Jun	09-May	<b>1.29</b> End of data (>4 days)	1.02 (18)	EqDr	27-May
1957	N/A	09-Jun	03-Jun	0.87 (0)	0.55 (2)	EqEq	06-Jun
1956	N/A	09-Jun	03-Jun	1.19 (2)	0.46 (7)	EqDr	06-Jun
1955	N/A	09-Jun	15-Jun	<b>0.41</b> 0.33 (10)	0.35 (1)	EqDr	12-Jun
1954	N/A	08-Jun	05-Jun	0.90 (2)	1.33 (5)	EqDr	07-Jun
1953	N/A	26-Jun	24-May	0.46 (1)	0.40 (3)	EqDr	10-Jun
1952	N/A	13-Jun	01-Jun	0.27 (5)	1.84 (0)	EqDr	07-Jun
1951	N/A	29-May	07-Jul	0.26 (3)	0.44 (2)	EqEq	18-Jun
1950	N/A	08-Jun	05-Jun	<b>0.76</b> 0.25 (9)	0.48 (0)	EqDr	07-Jun
1949	N/A	25-Jun	09-Jun	<b>1.31</b> 0.49 (1)	0.41 (2)	EqDr	17-Jun
1948	N/A	16-Jun	18-Jun	0.27 (4)	0.39 (15)	EqDr	17-Jun

**Table 3-1 Results. Years of this study are indicated in the farthest left-hand column. The transition date chosen from the 500-mb geopotential height criterion is in the second column, with no data gathered between 1948-1967. The chosen date for the first temperature selection criterion is in the third column, with the date**

**for the second criterion in the fourth column. The fifth column indicates the twenty-four-hour rainfall accumulation amount (in inches) for the significant rainfall event preceding the final chosen date, along with the number of dry days that elapsed between the rainfall event and the transition date (in parentheses). Bolded numbers in the fifth column show whether significant rainfall that occurred on the chosen transition day; if so, that amount is listed in inches. If rain occurred on the chosen transition day but it was not significant (i.e. it did not meet the 0.25-inch minimum threshold), it was not recorded. The sixth column illustrates the next significant twenty-four-hour rainfall accumulation event (in inches) after the final chosen date, along with the number of dry days that elapsed between the transition date and the rainfall event (in parentheses). The seventh column outlines the predicted coupling of ENSO/PDO, and what effect that should have on these temperatures and precipitation amounts. The eighth column indicates the final onset date chosen by this study.**

### 3.2 — DATA ANALYSIS

The aim for this data set was to compile parameters for the summer transition date for sixty-six years. Data that led to a transition date choice were found for all but three years, 1963, 1966 and 1967. Thus these years are excluded from the main statistics, and sixty-three years in total are analyzed.

The average transition date for the entire data set, 1948-2013, is 11 June. The median transition date for the set is also 11 June. Both of these dates fall after the accepted meteorological start date for summer, 01 June. The mode date is closer to meteorological onset at 07 June. June is, by far, the most common month for final transition dates: it boasts 85.71% of all chosen values (fifty-four out of sixty-three). May is a distant second, with 12.70% of all chosen transition dates (eight out of sixty-three), and July only has one transition date, accounting for the other 1.59% of the data set. Table 3-2 outlines the mean, median and mode of all chosen onset dates for each deterministic parameter. Table 3-3

illustrates the frequency and spread in chosen onset dates per individual parameter and for a final onset date. Figure 3.1 also depicts the frequency of onset dates, but further details the information by outlining the occurrence by calendar day. Table 3-4 shows the frequency of the implementation of the methodologies listed in Section 2.3.6 Data Accountability to choose a final transition date.

	500 mb Height (1968-2013)	Temperature Criterion 1	Temperature Criterion 2	FINAL CHOSEN DATE
MEAN	16-JUN	11-JUN	06-JUN	11-JUN
MEDIAN	14-JUN	12-JUN	06-JUN	11-JUN
MODE	19-JUN	08-JUN	15-JUN	07-JUN

**Table 3-2 Statistics of Onset Dates per Parameter, 1948-2013. Mean, median and mode of each parameter are listed by row, with each parameter listed by column. Final chosen date mean, median and mode can be found in the fourth column.**

	500 mb Height (1968-2013)	Temperature Criterion 1	Temperature Criterion 2	FINAL CHOSEN DATE
MAY	1	7	18	8
JUNE	41	58	46	57
JULY	4	1	2	1
SPREAD	38	42	59	45

**Table 3-3 Frequency and Spread of Chosen Onset Dates within the Analyzed Months of May, June and July. The May, June and July rows indicate the number of times an onset date was chosen in that month. The spread row shows the number of whole days between earliest chosen onset date and latest chosen onset date for an individual parameter. Each parameter is listed by column, with the final chosen date in the fourth column.**

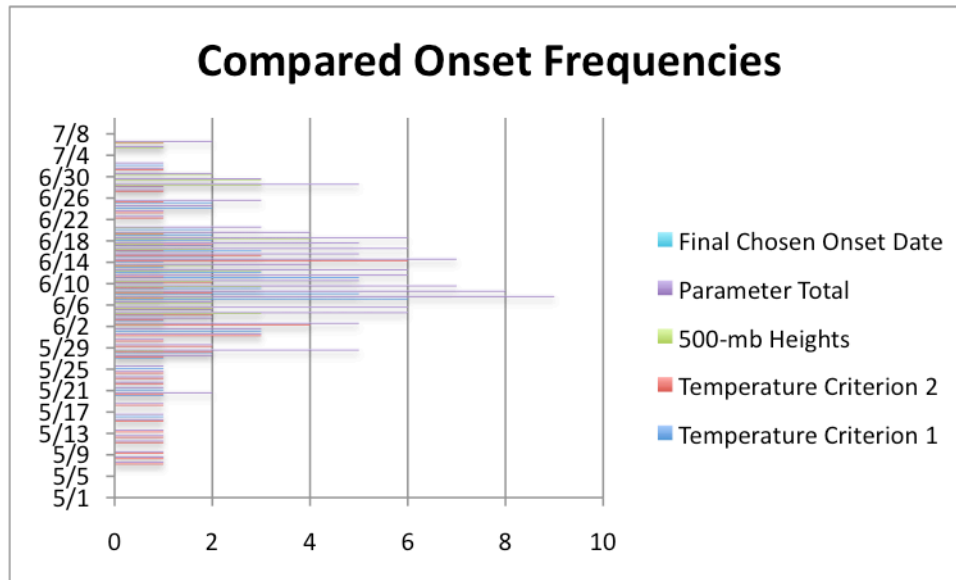


**Figure 3.1 Compared Frequencies of Chosen Onset Date Illustrated by Individual Parameter. Parameter Total is the sum of Temperature Criterion 1, Temperature Criterion 2 and 500-mb Heights. The frequency of choice is indicated along the x-axis, and the chronological onset date is located along the y-axis.**

	AVERAGE	OUTLIER	MEDIAN
YEARS	<b>29</b>	<b>10</b>	<b>2</b>

**Table 3-4 Frequency of Methodology Application for the Final Transition Date, 1968-2013. Average refers to a  $\pm$ ten-day average of all three variables. Outlier refers to an average of two days within a ten-day range, excluding one outlier beyond the ten-day maximum threshold. Median refers to years with all data points greater than ten days apart, leading to the choice of the middle onset value.**

Table 3-2 indicates a chronological continuum of summer transition dates per parameter. The second temperature criterion, 77.0°F (25.0°C) with at least ten of fifteen days having a temperature at, or exceeding, 82°F (27.8°C) leads to the earliest summer onset, at 06 June. The first temperature criterion, 70.0°F (21.1°C), and at least ten of fifteen days having a temperature at, or exceeding, 75.0°F (23.9°C) yields a moderating onset date between the second temperature

criterion and the 500-mb map data at 11 June. As 11 June is also the mean and median of the entire list of onset dates, this is an indicator that Temperature Criterion 1 data are the most pertinent for this study. 500-mb height data led to the latest summer onset dates, with a mean at 16 June. Importantly, the entire spread of the mean of the transition dates between parameters falls within ten days, or the space of one planetary wave. The spread of the median of the transitions dates is smaller, at eight days, and the spread of the mode of the transition dates is slightly greater, at eleven days. The criteria judged for summer onset dates were confined to a ten-day evaluation, so the mean and median of onset dates falling within this period validate experimental assumptions. Though the mode is outside of this period, the spread is only one day, which is still precise enough to accept the analyzed variables as valid.

It is clear from Table 3-3 that the parameter with the smallest range of values is the 500-mb height data set, indicating a more static, less volatile variable. Temperature Criterion 1 data showed more variability, and Temperature Criterion 2 data showed the most, at fifty-nine whole days between earliest and latest onset dates. Again, the Temperature Criterion 1 data are the most reliable in guiding the final chosen onset date: for May, June and July, the Temperature Criterion 1 data only had a maximum one-day spread from the final chosen onset date data frequency. Temperature Criterion 2 departed from the final transition date data most in the month of May, showing an earlier skew, and 500-mb heights had slightly higher July onset numbers, indicating a later skew.

Figure 3.1 compares the frequencies of onset dates between parameters. It includes a summation of parameter frequencies for onset dates and the frequency

of final chosen onset dates. The summed frequency of onset dates illustrates that no single date was chosen more than nine times across all examined variables, which strengthens the purpose of this study: no single variable can or will choose the same summer onset date annually.

Table 3-4 outlines the frequency of the different methodology application for choosing summer onset dates from 1968-2013. This time frame is chosen in order to include the 500-mb height data. Of the forty-six years examined, five years utilized only the 500-mb height data to secure a transition date, thus forty-one years are included in this table. 70.7% of all 1968-2013 summer onset dates were chosen using the averaging method, indicating that more than two-thirds of all years had transition dates that fell within ten days of one another. This method was the most accurate, as it utilized all three onset dates given by the three parameters. The outlier method and the median method have to exclude at least one date from one parameter, which fell outside of the ten-day maximum threshold. Thus the averaging method is the most holistic, and the percentage of its use helps to further validate the chosen summer onset dates in this time period.

Error is avoided in Table 3-4 by using the averaging method on the ten-day threshold, though conceivably, averaging may mask appreciable variability between onset dates. This error is assumed to be smaller, however, than the error inherent in the other two methods. Arguably, excluding the outlier date in the outlier method may neglect the most accurate variable, while averaging two variables that are potentially related in miscalculation. This method still uses two variables, though, which adds weight to its application. The median method is

assumed to be the most inaccurate, considering only one transition date is adequately utilized, and that date may be incorrect. The errors of the second and third method are still allowed in this study, due to their small sample size: only 24.4% of all onset dates used the outlier method, the less imprecise of the two, and only 4.9% of all onset dates used the median method, the more imprecise of the two.

### 3.2.1 – OSCILLATION ANALYSIS

El Niño Southern Oscillation, though it has three main modes, must also be examined during its transitional phases (i.e. La Niña becoming El Niño by fall, Neutral becoming La Niña by fall, etc.). Six transitional phases exist, along with three steady-state phases, where conditions remained the same throughout the course of a year (e.g. an El Niño year stayed El Niño that fall). According to the calculated findings of Ratley et al. (2002), steady-state conditions should lead to early-arriving summers, while transitional years should lead to late-arriving summers. Table 3-5 outlines the statistics for all nine conditions of ENSO, including the number of years of each phase in this data set and the expectation of the summer onset date following Ratley et al. (2002).

	NE/NE	NE/LA	NE/EL	LA/LA	LA/NE	LA/EL	EL/EL	EL/LA	EL/NE
NUMBER OF YEARS	22	3	10	6	6	4	1	7	7
MEAN	12-JUN	12-JUN	13-JUN	14-JUN	10-JUN	09-JUN	07-JUN	06-JUN	12-JUN
MEDIAN	12-JUN	12-JUN	15-JUN	14-JUN	10-JUN	08-JUN	07-JUN	08-JUN	15-JUN
MODE	12-JUN	NONE	18-JUN	NONE	NONE	06-JUN	07-JUN	13-JUN	NONE
INFLUENCE	EARLY	LATE	LATE	EARLY	LATE	LATE	EARLY	LATE	LATE

**Table 3-5 The Statistics of the Nine Phases of ENSO, 1948-2013. The first row lists the number of years spent in each phase in this data set. The second and third rows illustrate the median and mode for each condition, respectively. The fifth row outlines the qualitative summer onset date expectation from Ratley et al. (2002). The phases are indicated by the starting phase in October of one year, and the phase designated by the next fall, using Neutral (NE), La Niña (LA) and El Niño (EL).**

As seen in Table 3-5, steady-state Neutral phase is by far the most prevalent of this data set. It is also the most common type of ENSO phase noted since records began in the 1800s (“JMA SST ENSO Index,” [www.coaps.fsu.edu/jma](http://www.coaps.fsu.edu/jma)). Twenty-two years of this data set fell into steady-State Neutral, and thirty-five years in total fell in a condition of Neutral phase. El Niño and La Niña total phase type numbers were far fewer than Neutral, but had similar frequency one another: sixteen years and fifteen years in total, respectively. The earliest mean transition date noted was 06 June, which was in transitional year from El Niño to La Niña.

The expectations of early- and late-arriving summers did not appear to apply to these averages, as outlined by Ratley et al. (2002). The data set was affected by small samples, although arguably it was larger than the set of Ratley et al. (2002), and thus more statistically robust. For example, the Neutral to La

Niña group of data in this work was supposed to register a late-arriving summer: instead, it contained the exact same average onset date as the early-arriving expectation for steady-state Neutral. There were only three years involved in the mean, median and mode calculation for this phase, however, which could be the source for the assumed error of matching dates. The same principle applies to the steady-State El Niño phase, which held one of the earliest onset averages. Though the expectation was for an early onset date, only one year fell in this phase during the entire data set, which could have affected the onset outcome, even if it was in favor of scientific expectations. In addition, early onset dates do not necessarily indicate warmer total summer temperatures, making a direct correlation difficult to prove. A further listing of all years that fell into the nine phases of ENSO can be found in Table 3-6.

NE/NE	NE/LA	NE/EL	LA/LA	LA/NE	LA/EL	EL/EL	EL/LA	EL/NE
2013	1967	2009	1999	2011	1976	1987	2010	2003
2012	1954	2006	1975	2008	1972		2007	1992
2005	1949	2002	1974	2000	1965		1998	1983
2004		1997	1971	1989	1957		1988	1977
2001		1991	1956	1968			1973	1966
1996		1986	1955	1950			1970	1958
1995		1982					1964	1952
1994		1969						
1993		1963						
1990		1951						
1985								
1984								
1981								
1980								
1979								
1978								
1962								
1961								
1960								
1959								
1953								
1948								

**Table 3-6 The Years of the Nine Phases of ENSO, 1948-2013. Phases are indicated by the starting phase in October of a year, and the phase designated by the next fall, using Neutral (NE), La Niña (LA) and El Niño (EL).**

Pacific Decadal Oscillation, the chronologically longer scale of the two, is known to modulate the outcomes of El Niño Southern Oscillation (Birk et al., 2010). Due to the longevity of PDO, only two transitional years were found for this data set. The effects of the transition are not analyzed in the single year, because the physical changes that occur due to PDO phases take multiple years to be significant enough to be calculated. Table 3-7 outlines the years of PDO phases included in this study, along with the average final transition dates for each phase.

-PDO 1947-1976	+PDO 1977-1998	-PDO 1999-2013
10-JUN	13-JUN	10-JUN

**Table 3-7 PDO Phases and Average Summer Onset Dates from this Study. Phases are indicated by -PDO (low) and +PDO (high).**

Though the shift in average onset dates is small, it is clear that low PDO modes have a slightly earlier summer transition date than high PDO modes. The same mean onset date for the low PDO phases of 1947-1976 and 1999-2013 illustrates that the 500-mb height data absence and presence (respectively) still led to the same summer onset under PDO guidance. The sample sizes of these calculations were large enough to be indicative, as only three periods contained the entirety of this study. Therefore the onset dates of high and low PDO phases, while robust, are not highly variant: they fall within the space of one synoptic-scale wave.

Tables 3-8, 3-9 and 3-10 illustrate the mean, median and mode final transition dates chosen for the phases of PDO. Five out of the six coupling pairs of ENSO/PDO have no appreciable effect on temperature, so no correlation is expected between the dates. The ENSO phase with least variance between high and low PDO phases is El Niño, with the earliest average onset date of 07 June and the latest onset date of 12 June. Both Neutral and La Niña modes span the time frame of one planetary wave (ten days) between high and low PDO modes.

	-PDO 1947-1976	+PDO 1977-1998	-PDO 1999-2013
MEAN	05-JUN	15-JUN	12-JUN
MEDIAN	07-JUN	15-JUN	10-JUN
MODE	27-MAY	12-JUN	NONE

**Table 3-8 Statistics of Summer Onset Dates in ENSO Neutral Mode under PDO Phases. Phases are indicated by -PDO (low) and +PDO (high).**

	-PDO 1947-1976	+PDO 1977-1998	-PDO 1999-2013
MEAN	14-JUN	01-JUN	04-JUN
MEDIAN	13-JUN	01-JUN	03-JUN
MODE	17-JUN	NONE	NONE

**Table 3-9 Statistics of Summer Onset Dates in ENSO La Niña Mode under PDO Phases. Phases are indicated by -PDO (low) and +PDO (high).**

	-PDO 1947-1976	+PDO 1977-1998	-PDO 1999-2013
MEAN	12-JUN	10-JUN	07-JUN
MEDIAN	09-JUN	08-JUN	14-JUN
MODE	06-JUN	NONE	NONE

**Table 3-10 Statistics of Summer Onset Dates in ENSO El Niño Mode under PDO Phases. Phases are indicated by -PDO (low) and +PDO (high).**

La Niña varied more closely with El Niño in both high and low PDO phases, suggesting that Neutral has more definitively different phase effects in Missouri. Neutral is the most prevalent of all phases, so it had an ample data set that was not affected by small samples. This finding implies that the years of high ENSO activity, both El Niño and La Niña, are more closely correlated in their effects on the state of Missouri than the effects of the Neutral years. Moreover, there appears to be a continuum of a relationship between the phases: La Niña showed a closer relationship to El Niño, and El Niño showed a closer relationship

to Neutral. El Niño appears to be the moderating phase of the three for the choice of a summer onset date in Missouri, though it still falls within the space of one planetary wave between the two other modes.

According to Birk et al. (2010), the ENSO/PDO coupling that has a statistically significant impact on both temperatures and precipitation is El Niño in a high PDO phase. Of the high PDO phase years, though, the El Niño mean, median and mode onset dates displayed middling values in comparison to Neutral and La Niña in high PDO. El Niño in the high PDO phase of 1977-1998 appeared only five times, due to the influence of PDO helping to initiate Neutral and La Niña modes. When the five years (1982, 1986, 1987, 1991 and 1997) were examined more closely, they revealed an average summer onset date of 10 June. This was the scientific expectation (according to Birk et al. (2010)), as an earlier-starting summer could signal a warmer one, but the average is only twenty-four hours earlier than the overall average summer onset date of this study, 11 June. Therefore the finding is likely not appreciable.

ENSO/PDO effects that lacked sizeable results in this study could also be found in the predicted wet and dry conditions from ENSO/PDO coupling. Table 3-11 illustrates the findings for wet and dry conditions, as expected from ENSO/PDO-tied influences.

	Dry Conditions Expected: Rainfall Before Onset	Dry Conditions Expected: Rainfall After Onset	Wet Conditions Expected: Rainfall Before Onset	Wet Conditions Expected: Rainfall After Onset
Average Number of Days Between Significant Rainfall Events	5.03	6.97	5.40	7.00

**Table 3-11 Coupled-Effect Expectations of ENSO/PDO on Rainfall in Missouri. Data indicate average number of whole dry days before and after final chosen summer onset for 1948-2013.**

Table 3-11 depicts forty-nine years of this study; the excluded years were those in which ENSO/PDO coupling selected for equal chances of dry and wet conditions. The expectations of a drier regime after the onset of summer remained true in this table, as significant rainfall events were more prevalent before the final chosen onset date. However, there is almost no discernible difference between expected dry and expected wet years: average significant rainfall event days between dry and wet years showed less than a half-day (0.5) discrepancy.

Potential errors introduced by the utilization of ENSO and PDO include the use of the JMA SST ENSO Index, which is a standard used in other academic papers. However, there are different definitions of ENSO phases, and though steady-state phases are more likely to have consensus, transition years have more incongruity between definitions. Considering no appreciable difference was found between early and late onset dates in transitional versus steady-state years

and between coupling effects, it is possible that the index used was not most indicative of the effects actually seen in the state.

### 3.2.2 — UPPER-AIR MAP ANALYSIS

The 500-mb height maps produced the latest-arriving mean, median and mode onset dates in each respective category across all three analyzed parameters, indicating a later-skewing set of data. The average start date outcome, following the 500-mb height condition, was 16 June. The median was 14 June. The mode was closest to the astronomical start date of summer, at 19 June. The frequency of onset dates according to the criteria set for the 500-mb data is found in Figure 3.2.

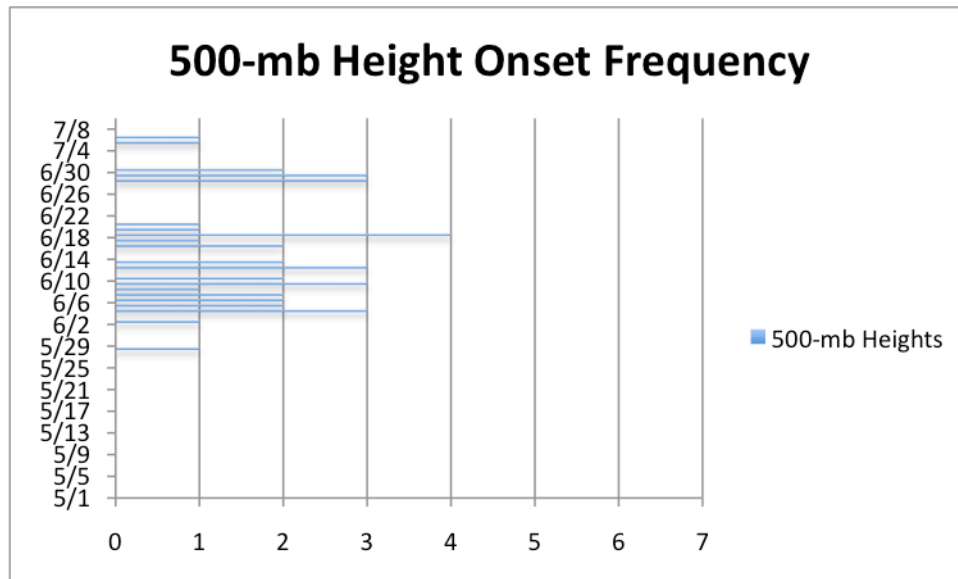


**Figure 3.2 Frequency of Onset Date Dictated by 500-mb Heights. The frequency of onset is indicated along the x-axis, and the chronological onset date is located along the y-axis.**

As seen in Figure 3.2, only one transition date was identified in the month of May for the entire data set, 1968-2013. The later skew of the 500-mb data also created more July onset dates than any other parameter, at four. Only one transition date was selected as many as four times; most often, a specific transition date appeared only once.

In meteorological analysis, upper-air conditions are the source of surface effects (Ahrens, 2012). Since the temperature and precipitation data gathered from Jefferson City were surface data (i.e. two-meter temperatures and surface rain gauge observations), it is important to assert that the surface data were independent of 500-mb heights. To combat the potential of analyzing correlated data, contingency tables (Table 3-12 and Table 3-13) show the relationship of Temperature Criterion 1 and Temperature Criterion 2 to the 500-mb geopotential height onset dates.

Number Total % Row % Column%	Within 24 Hours of Temperature Criterion 1	Not Within 24 Hours of Temperature Criterion 1	TOTAL
MAY	0 0 0 0	1 2.38 100 2.78	1 2.38
JUNE	6 14.29 15.79 100	32 76.19 84.21 88.89	38 90.48
JULY	0 0 0 0	3 7.14 100 8.33	3 7.14
TOTAL	6	36	42
$\chi^2$ MAY JUNE JULY TOTAL $k=(r-1)(c-1)=2$	0 0.0603 0 0.0603	0.0239 0.0100 0.0716 0.1055	

**Table 3-12 Contingency Table Comparing 500-mb Heights to Temperature Criterion 2. Independent y-axis compares 500-mb geopotential height onset dates to potentially dependent x-axis of Temperature Criterion 1 onset dates. Categorical columns are chosen to show a relationship if onset dates are within twenty-four hours of one another. Degrees of freedom, k, are calculated by (row – 1) multiplied by (column – 1).**

Number Total % Row % Column%	Within 24 Hours of Temperature Criterion 2	Not Within 24 Hours of Temperature Criterion 2	TOTAL
MAY	0 0 0 0	1 2.38 100 2.56	1 2.38
JUNE	3 7.14 7.89 100	35 83.33 92.11 89.74	38 90.47
JULY	0 0 0 0	3 7.14 100 7.69	3 7.14
TOTAL	3	39	42
$\chi^2$ MAY JUNE JULY TOTAL $k=(r-1)(c-1)=2$	0 0.0301 0 0.0301	0.0059 0.0020 0.0158 0.0237	

**Table 3-13 Contingency Table Comparing 500-mb Heights to Temperature Criterion 2. Independent y-axis compares 500-mb geopotential height onset dates to potentially dependent x-axis of Temperature Criterion 2 onset dates. Categorical columns are chosen to show a relationship if onset dates are within twenty-four hours of one another. Degrees of freedom, k, are calculated by (row – 1) multiplied by (column – 1).**

Table 3-12 and Table 3-13 illustrate the potential relationship between 500-mb height onset dates and the two temperature criteria onset dates. Forty-one years of this study were analyzed in the contingency tables, to ensure all variables were present. The chosen threshold for a relationship between the parameters was twenty-four hours, which, if seen, would indicate a choice that varied jointly with 500-mb heights.

For these tables, a numerical continuum was changed into a discrete categorical variable: the range of chosen onset date was reassigned to a “yes” and “no” category.

The formula used to calculate the chi-square portion of the table was the following:

$$\chi^2 = \sum \frac{(\text{observed} - \text{expected})^2}{\text{expected}}$$

where the chi-square value is the sum of the squares of the independent normal random variables, and k, the degrees of freedom, is a positive integer (“Two-Way Tables and the Chi-Square Test,” [www.stat.yale.edu](http://www.stat.yale.edu)). Taking the degrees of freedom (in this case, two) and the chi-square value and comparing to a chi-squared distribution table revealed that the cutoff level of significance, where  $p \leq 0.05$ , was not reached by the values calculated in this study.

That meant that the null hypothesis in both Table 3-12 and Table 3-13 was not able to be rejected: there is a greater than 5.00% chance that the two variables occur randomly, i.e. there is no significant relationship between the two. Importantly, this applies to when 500-mb height transitions are within twenty-four hours of the temperature criteria, and when they are not. This indicates that there is no direct or indirect joint variation between the parameters, so they are independent of one another. Thus the 500-mb height parameter would need to remain in any further summer onset study, as the outcomes of surface temperature data cannot directly relate to upper-air analysis.

In theory, the 500-mb data should be the most useful for this study, as upper-air analyses are not subjected to surface observation errors and influences.

The slightly later skew of the onset dates at 500-mb could be considered more accurate than the temperature parameters, especially since the mean, median and mode of the 500-mb data fell closer to the astronomical start date of summer (usually 20 or 21 June) than the meteorological one (at 01 June). However, there were errors inherent in the 500-mb data collection. Years before 1968 were rejected for this study due to prevalence of hand-drawn mapping and sparse data observations. Though computers now automate the mapping of 500-mb data, interpolation must still be processed between observational sites, introducing intrinsic error. For this study, the daily errors created in the 500-mb maps were considered small enough to justify use on multiday scales. The contours alone covered a distance greater than 5,000 kilometers, which made evaluation errors small, as the state of Missouri is less than 400 kilometers across (“50 State Rankings for Size,” [www.netstate.com](http://www.netstate.com)).

When final chosen dates were reevaluated without the 500-mb data, the mean of the onset dates shifted only seventy-two hours. 08 June became the new onset date. Since this date still fell within the time scale of one synoptic wave, it is clear that the presence or absence of the 500-mb data did not produce a skew too large to be useful in this study.

### 3.2.3 — TEMPERATURE DATA ANALYSIS

Ratley et al. (2002) found that daily mean temperature (Temperature Criterion 1) was the most reliable variable in earlier research: the final chosen date and the calculated daily mean temperature onset date fell within two days of one another for eighteen of twenty years examined.

This study found a similar pattern. The daily mean temperature was one of the strongest variables examined, due assumedly to its holistic look at the surface conditions of one calendar day. The average onset of the mean temperature, or Temperature Criterion 1, was the exact same as the average onset for final chosen transition dates: 11 June. 12 June was the median date for this criterion, and 08 June was the mode. The average frequency of the onset dates for Temperature Criterion 1 can be found in Figure 3.3.

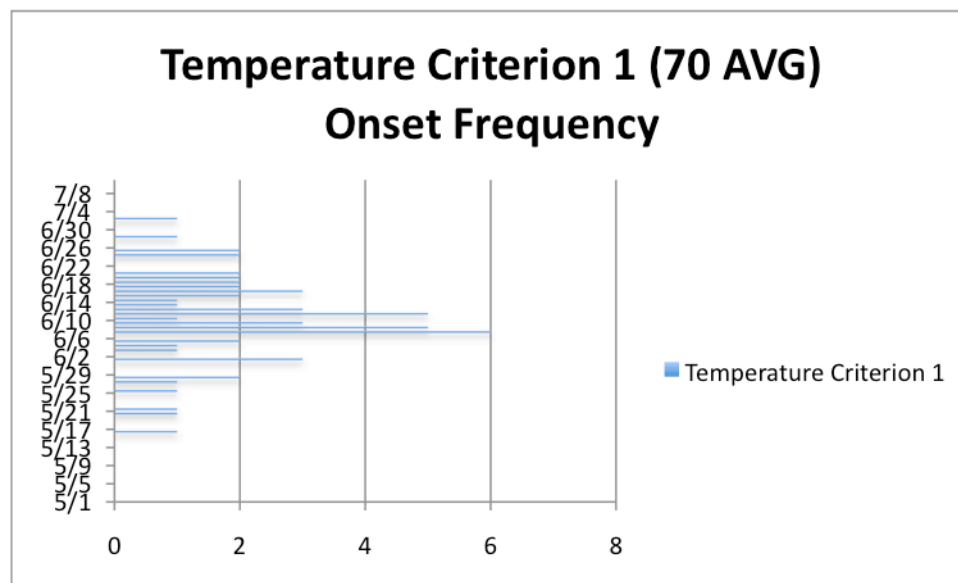


**Figure 3.3 Frequency of Onset Date Dictated by Temperature Criterion 1: The First Date of a Fifteen-Day Consecutive Period Where the Mean Temperature Exceeds 70.0°F (21.1°C), and at Least Ten of Those Fifteen Days Have a Temperature at, or Exceeding, 75.0°F (23.9°C). The frequency of onset is indicated along the x-axis, and the chronological onset date is located along the y-axis.**

Figure 3.3 shows that no single onset date was identified more than six times, but that the dates overall have a quasi-normalized distribution, with a spread very similar to that of the final chosen onset dates. Seven (eight) transition dates fell in May, fifty-eight (fifty-seven) dates fell in June and forty-

two (forty-five) dates fell in July for Temperature Criterion 1 (final chosen onset date).

In comparison, the second temperature criterion, which examined maximum daily temperatures, was slightly less reliable overall in this study, if the spread between a parameter and the final onset date is chosen as a mark of accountability; this was an interesting finding, as most colloquial definitions of summer attribute onset to warm daily high temperatures. The average onset date for the second criterion is 06 June, which falls within the space of one synoptic-scale wave from the average final chosen onset date, but is earlier than Temperature Criterion 1. The median for Temperature Criterion 2 is also 06 June. The mode of the second temperature criterion is 15 June, indicating some earlier-skewing onset dates affected the mean and median. Figure 3.4 illustrates the average frequency of the onset dates for Temperature Criterion 2.

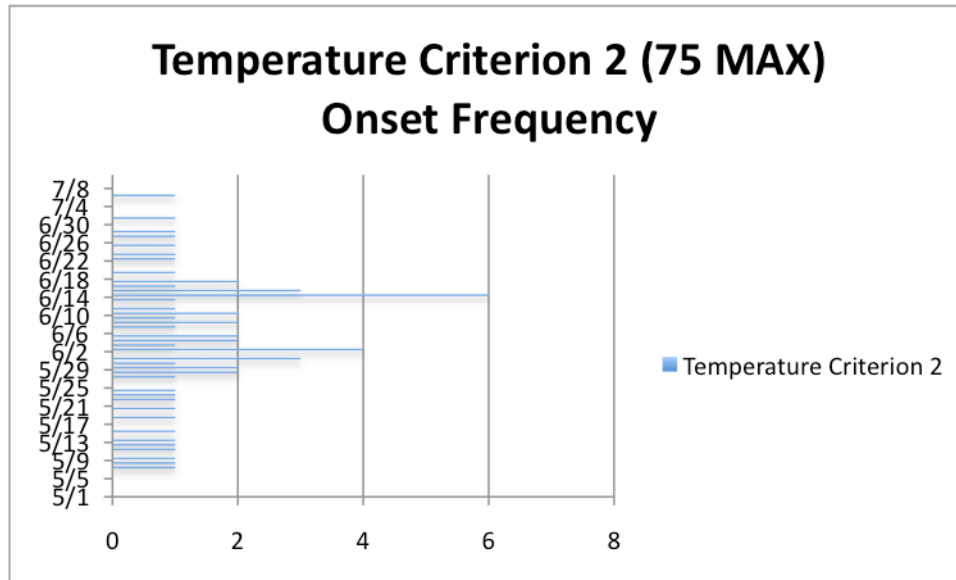


**Figure 3.4 Frequency of Onset Date Dictated by Temperature Criterion 2: The First Date of a Fifteen-Day Consecutive Period Where the Maximum Temperature Exceeds 77.0°F (25.0°C) and at Least Ten of Those Fifteen Days Have a Temperature at, or Exceeding, 82°F (27.8°C). The frequency of onset is indicated along the x-axis, and the chronological onset date is located along the y-axis.**

Figure 3.4 shows the same maximum repetition of an onset date as Figure 3.3, at six, but Figure 3.4 depicts more single-frequency onset dates than Temperature Criterion 1, with an earlier (May-leaning) spread. Due to the fact that Temperature Criterion 2 data fell further from the final chosen onset data, Criterion 1 proved to be the more beneficial to this study and the outcome of identifying a summer transition date.

It is conceded that there are multiple potential errors in the temperature data analysis. The methodology of averaging two surrounding days' temperatures to fill a gap in an otherwise complete data set introduces known error. The incidence, however, was rare and considered unimportant across the course of the sixty-six years of this study (which led to 4,686 daily temperature recordings

for maximum temperatures alone). Jefferson City was the standard for station reporting in this study, though occurrence of measurement calibration is unknown. As temperature data fell within principally expected typical temperatures for the months examined, though, these errors were considered to be miniscule. Finally, the process of collecting temperature data by hand also introduced the possibility of human error, as temperatures for Jefferson City had to be input by hand into analysis packages. Again, as data fell within an essentially expected range, this type of error was considered small enough to be inconsequential to the study.

#### 3.2.4 — PRECIPITATION DATA ANALYSIS

The methodology used to quantify precipitation data by Ratley et al. (2002) was altered slightly during this research. While both studies looked for the frequency between significant precipitation events ( $>0.25''$ ) to validate summer onset date choices, Ratley averaged precipitation data back to the last significant event in April up to the significant event immediately preceding the chosen transition date (Ratley et al., 2002). The same technique was applied to average significant rainfall events immediately after the onset date until the last event prior to 01 September.

From the research done by Ratley et al. (2002), only one single summer transition date fell in May, one fell in July and all others were in June. In this study, dates prior to 1 May or after 10 July were excluded, so a new approach to significant precipitation event frequency was applied. The single closest significant precipitation events, both before and after the transition date, were

the ones recorded (reference Table 3-1). As predicted, significant precipitation events occurred more often before the summer onset date, as compared to after it. The average number of consecutive whole dry (or insignificant rain) days before the chosen transition date was 5.24, and the median number was 4 days. After the chosen onset date, the average number of whole dry (or insignificant rain) days increased to 6.91, with a median of 6 days.

The findings of the precipitation data fell in line with scientific expectation, as the anticipated drier periods of the summer scheme appeared after the final chosen transition date. The mode for both sets of data is zero, i.e. significant rainfall occurred on the day immediately before or after the chosen final date. It is of interest to note that, for fourteen chosen onset dates, significant rainfall occurred on the chosen date, as can be seen in column five of Table 3-1. The high incidence rate of rainfall on the chosen transition date may be an indicator that the last spring synoptic-scale frontal system was passing before summer settled into the area, a pattern that repeated over multiple years.

The occurrence of “End of data” days, which introduced known error, was seldom: it only happened four times before the chosen date, and two times after, so these data are still included, as the error tendency was small. The same type of reporting errors that applied to temperature data are relevant to precipitation data, too: but errors from station reporting and human recording are considered minute on multiyear scales.

### 3.2.5 – COMPARATIVE ANALYSIS

Ratley et al. (2002) found that in 45% (nine years out of twenty) of the 1981-2000 data set, summer onset dates fell within three to five days of one another. When they did not, Ratley et al. (2002) utilized averaging methodologies very similar to the ones in this research to include useful data and to exclude outliers. Their twenty-year mean was calculated to be 15 June, which most closely aligns with the statistical outcome of the 500-mb height data of this study. 60% of the onset dates (twelve years out of twenty) chosen by Ratley et al. (2002) fell between 10-20 June, with 20% (four days out of twenty) lying both before and after that time period. 65% of the onset dates fell between 05 and 25 June. Therefore Ratley et al. (2002) argued that the set of data analyzed by that work was in a normal distribution, as would be expected by Hart and Grumm (2001). Ratley et al. (2002) chose a final onset date within four days of the date chosen by this study (15 June versus 11 June, respectively).

Using the same formula as Ratley et al. (2002) to calculate distributions, +/- ten calendar days, the distributions found in this research are relatively normal. Figures 3.5, 3.6, 3.7, 3.8 and 3.9 illustrate the departure of the results of this study from the normalized distributions expected.

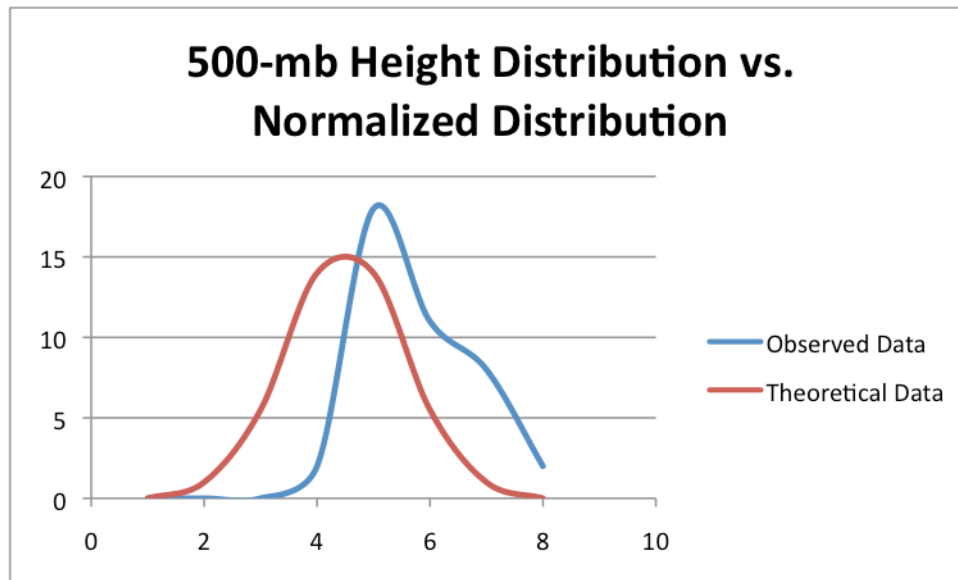


**Figure 3.5** Frequency of Onset Date Dictated by 500-mb Heights as Compared to a Theoretically Normalized Distribution. The chronological date is binned into multiples of eight on the x-axis, and the frequency of the onset date is indicated on the y-axis.

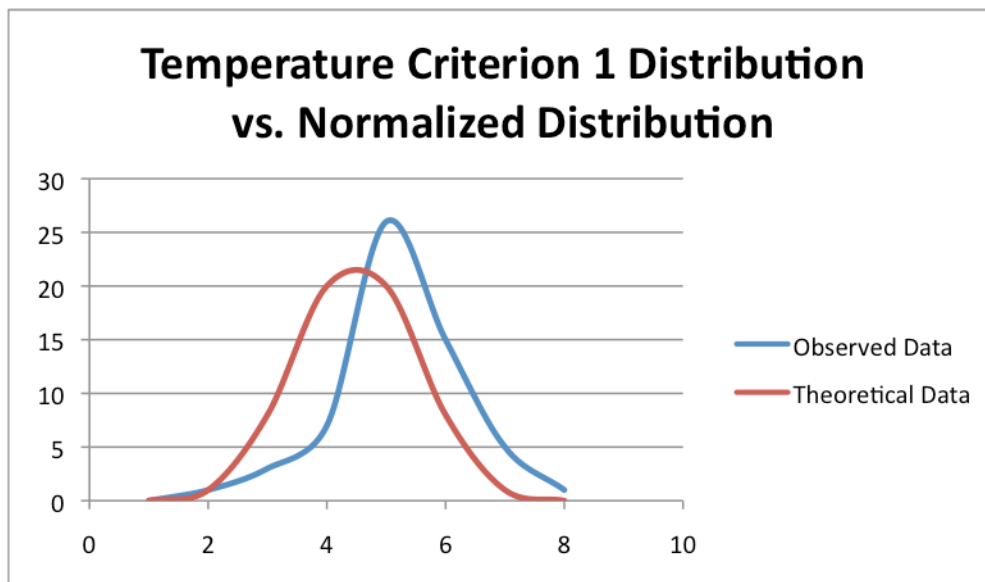


**Figure 3.6** Frequency of Onset Date Dictated by Temperature Criterion 1 as Compared to a Theoretically Normalized Distribution. The chronological date is binned into multiples of eight on the x-axis, and the frequency of the onset date is indicated on the y-axis.

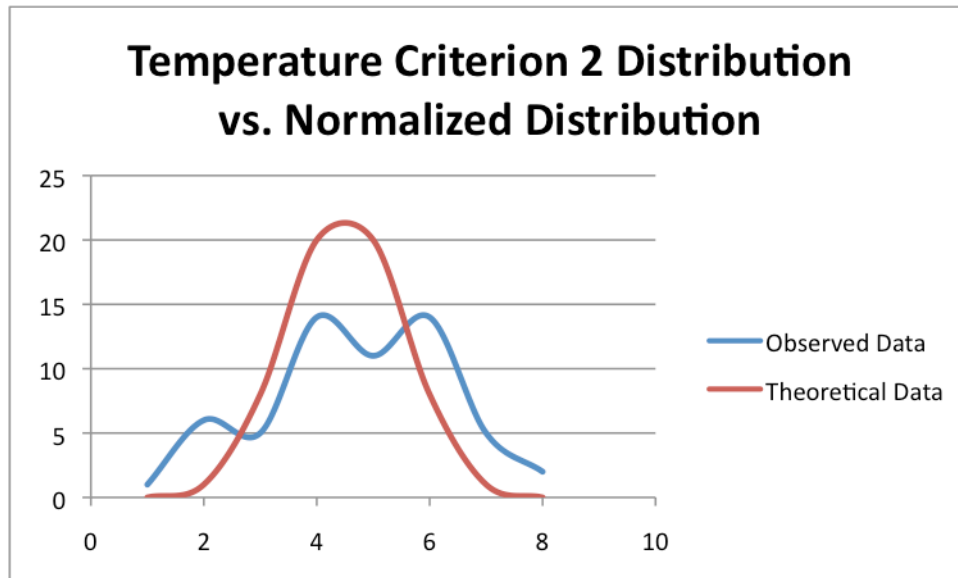


**Figure 3.7** Frequency of Onset Date Dictated by Temperature Criterion 2 as Compared to a Theoretically Normalized Distribution. The chronological date is binned into multiples of eight on the x-axis, and the frequency of the onset date is indicated on the y-axis.

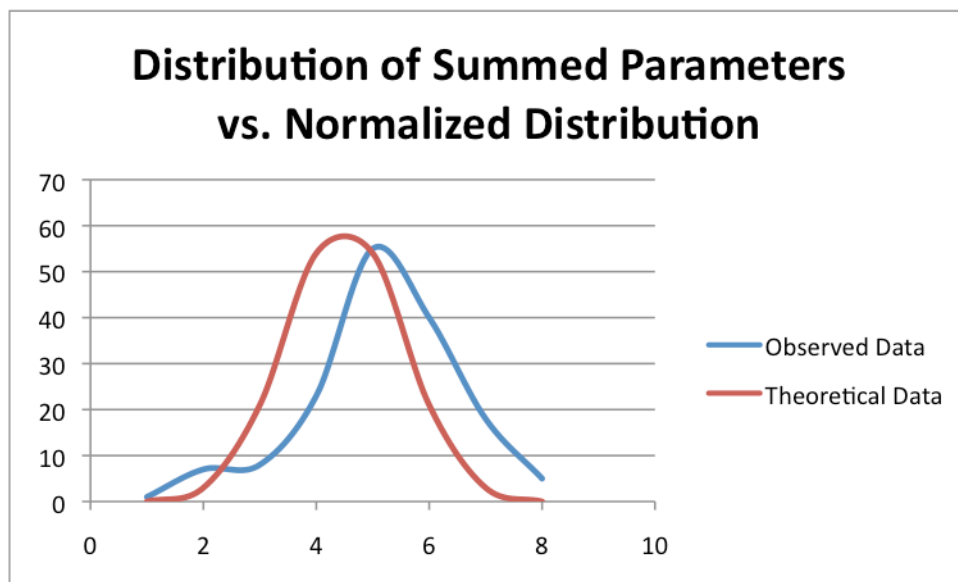


**Figure 3.8** Frequency of Onset Date Dictated by a Summation of the Three Analyzed Parameters of 500-mb Heights, Temperature Criterion 1 and Temperature Criterion 2 as Compared to a Theoretically Normalized Distribution. The chronological date is binned into multiples of eight on the x-axis, and the frequency of the onset date is indicated on the y-axis.

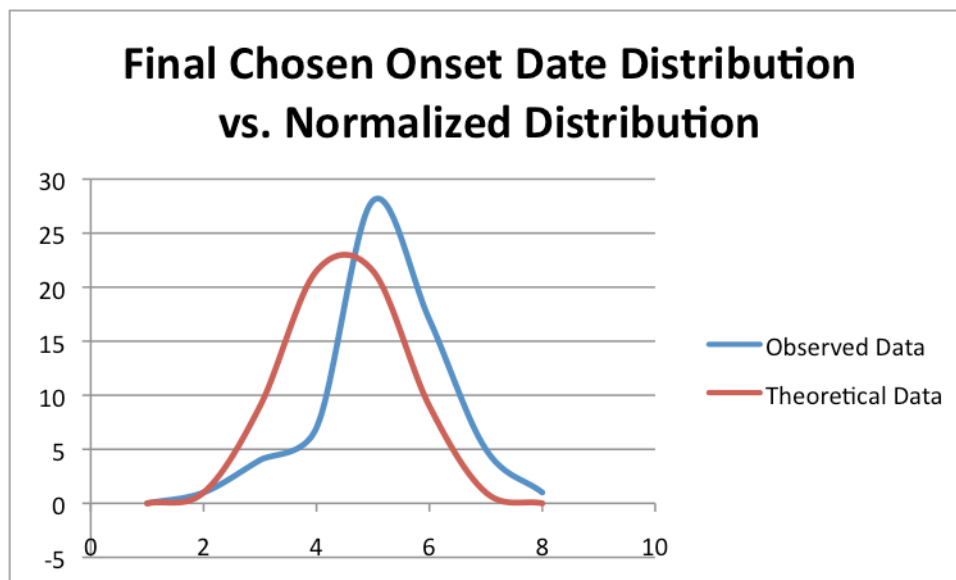


**Figure 3.9** Frequency of Final Chosen Onset Date as Compared to a Theoretically Normalized Distribution. The chronological date is binned into multiples of eight on the x-axis, and the frequency of the onset date is indicated on the y-axis.

Bins of eight were chosen for each of the theoretical distributions due to calculations from Sturges' Formula, which assumes a normalized distribution with sample sizes greater than thirty ("ModelAssist for ModelRisk," [www.VOSEsoftware.com](http://www.VOSEsoftware.com)). It is evident from Figures 3.5 – 3.9 that the distributions of data collected and analyzed in this study are quasi-normalized. All data from this study are still largely parabolic in nature, with a late-leaning propagation. Though Temperature Criterion 1 shows a growth rate more exponential than that of the normalized distribution, Figure 3.6 depicts an observed distribution closer to normal than the other two parameters, 500-mb heights and Temperature Criterion 2. This reasserts the importance of Temperature Criterion 1 in determining a summer onset date.

The error inherent in choosing methodologies to assign summer onset dates is apparent in Figure 3.8, as the summed parameters interestingly led to a very normalized distribution pattern for onset dates. The pattern seen in Figure 3.8 exhibits the same characteristics of the rest of the data (namely, later-propagating), but the overall distribution shape is almost ideal. This sum of parameters, however, also benefitted from having a larger sample size, and thus the onset date of one year is more minimized, should it be an outlier to an otherwise normalized distribution. Figure 3.7 must also be addressed, as it demonstrates an almost ideal normalized distribution, save for a peak point. It is possible that aforementioned errors (namely station reporting and calibration) led to a decrease in frequency for onset dates in that bin. Means were recalculated for each parameter, but one normalized distribution was used, so the propagation error apparent in every figure may be related to graphing, instead of an actual reflection of the data.

Ratley et al. (2002) identified a standard deviation of ten days. This study is similar: a standard deviation was calculated to be 9.80 days, rounded to ten for ease of computation. The period 02 June to 21 June ( $\pm 10$  days from the 11 June mean) encompassed forty-seven onset dates out of sixty-three years from 1948-2013, or 74.60% of the data. This reaches beyond the threshold of a normal distribution, which seeks 68.27% of the entire data set. The higher frequency of data within this grouping created a steeper growth rate than that of a theoretically normalized set of data. Eight onset dates lie chronologically before this set (seven in the first standard deviation, one in the second), which would exhibit characteristics of an almost normalized data distribution, if not for the

higher middle concentration. The same applies to the later set of onset dates: eight onset dates lie chronologically after the main set (seven, again, in the first standard deviation, one, again in the second), which aligns almost precisely with a normal distribution. In order to attain a normalized distribution overall, two more onset dates would have to lie on both sides of the main set, taken from the forty-seven, to lessen the slope of the graph.

A table of the differences in the chosen final onset date between this research and Ratley et al. (2002) during 1981-2000 can be found in Table 3-14.

Year	Chosen Date	Ratley et al. (2002) Chosen Date	Discrepancy (Whole Days Between)
2000	10-Jun	01-Jul	20E
1999	03-Jun	19-Jun	15E
1998	23-May	17-Jun	24E
1997	18-Jun	19-Jun	0E
1996	22-Jun	13-Jun	8L
1995	15-Jun	15-Jun	0, EXACT
1994	12-Jun	11-Jun	0L
1993	12-Jun	10-Jun	1L
1992	24-Jun	28-Jun	3E
1991	22-May	21-May	0L
1990	12-Jun	06-Jun	5L
1989	20-Jun	19-Jun	0L
1988	09-Jun	10-Jun	0E
1987	07-Jun	05-Jun	1L
1986	08-Jun	13-Jun	4E
1985	07-Jul	29-Jun	7L
1984	07-Jun	03-Jun	3L
1983	22-Jun	20-Jun	1L
1982	26-Jun	27-Jun	0E
1981	15-Jun	21-Jun	5E

**Table 3-14 Differences in Chosen Final Onset Date Between this Research and Ratley et al. (2002) during 1981-2000. The fourth column illustrates number of whole days that elapsed between the chosen date of this research and the chosen date by Ratley et al. (2002). A zero (0) indicates that the chosen dates fell within twenty-four hours of one another. Numbers in the fourth column are qualified with a marker to show that this research chose the summer onset date earlier (E) or later (L) than Ratley et al. (2002).**

The two analyses gave final dates that were an average of 2.2 days apart. As seen in Table 3-14, five transition days (25%) fell within twenty-four hours of one another. Thirteen transition days (65%) fell within five days of one another, still within the frame of one synoptic wave. Seventeen days (85%) of the data computed by this study fell within ten days, or one planetary wave, of the Ratley et al. (2002) outcomes. The data utilized in this research chose an earlier

transition date 45% of the time (nine days of the data set), even if only by twenty-four hours. This study also chose a later onset date 50% of the time (ten days), and chose the exact same transition date once, in 1995. The largest spread between chosen onset dates was 1998, with twenty-four days between.

The change in multiple parameters likely led to the discrepancies between this work and the work done by Ratley et al. (2002), though the differences are not significant in the overall analysis. The standard deviation of this study overall was calculated to be 9.8 days, but there was a discrepancy between the final onset date standard deviation and the standard deviations of the individual parameters. Had the individual standard deviations been implemented, the figures may have shown a more normalized distribution, as was the scientific expectation. In addition, as the spread between the final chosen onset dates of this study and the chosen onset dates of Ratley et al. (2002) grew at the end of the data examined by Ratley et al. (2002), there is also the potential for initial reporting error that may have affected the analysis by Ratley et al. (2002), as the previous authors wrote during a time sensitive to the reporting of that data.

## Chapter 4 CONCLUSIONS

The aim of this research was to strengthen the study conducted by Ratley et al. (2002). First, the methods used by the authors Ratley et al. (2002) were reevaluated and reinterpreted: in some cases, no changes were made, while in others, approaches were altered, in order to make more mathematically and logically strong arguments. The multiannual scope of the data coverage was enhanced, taking a data set from 1981-2000 and expanding it both forward and backward in time, from 1948-2013. Within each year, the months analyzed for a spring to summer transition were minimized, in order to fine-tune the process of identifying a summer onset date.

The overall chosen summer onset date changed from the work first published by Ratley et al. (2002). The previous authors argued that their research produced a normalized distribution around an average transition date of 15 June. This research identified 11 June as the average transition date, with a quasi-normalized distribution across all parameters, including the final onset dates, which were chosen using prescribed methodologies that were a time function of one planetary wave, or ten days. The use of the ten-day threshold ensured larger-scale data were captured, though often, small discrepancies between variables fell within the smaller time frame of one synoptic-scale wave (up to seven days), making the analysis robust. The four-day difference between these two average

dates from Ratley et al. (2002) and this study fell within the time scale of an average synoptic wave, for example, which indicates that the methodologies approached by the two studies strengthen one another, and show consensus. Moreover, seventeen out of twenty onset dates between Ratley et al. (2002) and this work align within ten days of one another, leading to an appreciable 85% agreement. In the three years that show marked inconsistency in onset date (1998, 1999 and 2000), a time-sensitive analysis of the research likely led to the later onset dates chosen by Ratley et al. (2002)

Beyond the scope of the work done by Ratley et al. (2002), the oscillation selection chosen by this work implemented the conclusions of recent work (notably Birk et al., 2010) about the coupling effect of El Niño Southern Oscillation with Pacific Decadal Oscillation. In examining the intensifying effect of ENSO/PDO stages, Neutral phases distinguished themselves from El Niño and La Niña phases, though all phases and phase-coupling effects had minimal variance, creating multiyear averages within a ten-day specified time frame. Even when dry and wet seasonal expectations were compared in the ENSO/PDO coupling framework, outcomes did not vary enough to create substantial onset changes.

The most important parameter analyzed in this work was Temperature Criterion 1, or the first date of a fifteen-day consecutive period where the mean temperature exceeds 70.0°F (21.1°C), and at least ten of those fifteen days have a temperature at, or exceeding, 75.0°F (23.9°C). The Temperature Criterion 1 data exhibited an almost ideal normalized distribution, with a spread of onset frequency the closest in equivalence to those of the final chosen onset dates of

any parameter. This temperature criterion took into consideration the daily maximum and minimum temperature for each day of the data set, creating a more well-rounded moment for analysis than that of the Temperature Criterion 2 data or the 500-mb maps. In fact, the mean Temperature Criterion 1 date was exactly the same as the mean final chosen transition date, at 11 June.

The 500-mb geopotential height contours were of second-most importance, due to the fact that upper-air analyses are removed from the potential inaccuracies of surface data. The upper-air contours were also shown to have no significant relationship to the surface temperature data, making the contours an independent and necessary parameter in the analysis of summer onset dates, as they cannot be inferred from surface measurements. The 500-mb maps created a later data skew, closer to that of the astronomical start of summer than any other parameter, which were balanced by the earlier skew of Temperature Criterion 2 data.

The second temperature criterion, or the first date of a fifteen-day consecutive period where the maximum temperature exceeds 77.0°F (25.0°C) and at least ten of those fifteen days have a temperature at, or exceeding, 82°F (27.8°C), held the least importance in creating a spring-to-summer transition date. This was unexpected, as most colloquially customary definitions of summer would include the necessity of warm daily high temperatures. Due to its low importance, the second temperature criterion could arguably be eliminated from future studies on this subject. This work argues for its presence, though, as it provided a lower chronological bound to balance out the 500-mb data.

## **Chapter 5 APPLICATIONS OF FINDINGS**

The findings of this research outline a focused ten-day transitional period between spring and summer. The shift between seasons, though single onset dates were chosen, tended to lie within ten days of one another throughout multiple years, as they were slightly influenced by ENSO and PDO phases and phase-coupling effects. The ability to create a long-range summer transition forecast for the West Central Plains of Missouri based on the dates identified in this research, which follow the ENSO/PDO rubric, is a competitive advantage to a forecaster.

Missouri is still a largely agricultural state, with few urban centers interspersed, creating a population density in the lower half of all U.S. states (U.S. Census Bureau, 2011). Agricultural products account for 377 billion dollars in exports from Missouri each year (“2013 Missouri Exports,” Missouri Department of Economic Development). Thus the number of heating days, number of cooling days, daily maximum and minimum temperature, amount of precipitation and frequency of precipitation are all forecasting interest factors, as they directly affect the agricultural sector. Recent studies indicate that Americans receive more than fifty percent of all of their weather knowledge through their local television weather broadcasters. As these broadcasters are usually viewed as resident station scientists, they are placed in an ideal position to communicate climatic knowledge to their audiences (Nese et al., 2012). As explained by Pennesi

(2011), local climatic forecasts are especially important in supporting the resilience and hardiness of rural communities. Thus it is of utmost importance for Missouri weather broadcasters to utilize information to help sustain Missouri agricultural interests.

Although it would be most prudent for Missouri's local National Weather Service offices (specifically in Kansas City, Springfield and St. Louis) to incorporate the findings of this data as baseline indicators for summer onset dates, local broadcast markets can capitalize on any lack of application by utilizing these parameters on an individual basis. This information will be most accessible to viewers when generalized: i.e., when all interests for the expectations of the seasons are considered. Agricultural interests, while of very high importance for weather forecasting in Missouri, likely have different seasonal expectations than those of tourism and entertainment, or those of a mathematically-driven meteorological definition. In order to encompass all viable summer onset definitions, it would be most advantageous to apply this research in an elongated time frame. As this study identified a ten-day average transitional period across the analyzed parameters, implementation of this research for different interests would dictate a slightly larger window. Two weeks, or fourteen days, would encompass roughly two synoptic-scale waves. Forecasting a summer transition period of two weeks would likely include all needed interests, while ensuring enough synoptic variability to capture the change.

Arguing for the applicability of this research, a case study can be made for the spring/summer transition of 2015. As of March 2014, the National Climatic

Data Center (NCDC) issued an El Niño Watch, with the potential to develop El Niño conditions by the summer or fall of 2014 (“El Niño/Southern Oscillation,” [www.ncdc.noaa.gov](http://www.ncdc.noaa.gov)). As of May 2014, the chance of a fall El Niño event increased from fifty percent to sixty-five percent.

Spring/summer conditions for 2014 are in Neutral phase. The planet has maintained steady-state Neutral since 2011, according to the JMA SST ENSO Index. If El Niño conditions do develop in the fall of 2014, the spring of 2015 will be a transitional year, indicating a late-onset summer. The NE/EL (Neutral to El Niño) phase has an average summer onset date of 13 June, a median onset date of 15 June and a mode onset date of 18 June. However, if El Niño conditions do not develop, the planet will again have a steady-state Neutral year. The NE/NE (steady-state Neutral) phase is expected to have an early transition date. NE/NE has an average summer onset date of 12 June, a median of 12 June and a mode of 12 June. Low PDO mode, which is expected to continue through 2015, would actually indicate a slightly earlier start date for NE/EL (07 June), compared to a slightly later onset date for NE/NE (12 June).

Although the basic statistics of the two phases differ under ENSO and PDO, the enlarged two-week chosen transitional period for forecasters would only be separated by one day, if the average ENSO onset date is used as the anchoring parameter. El Niño conditions by the spring of 2015 would create a summer transition period from 07 June to 20 June, with 13 June falling as the seventh day in the period. Steady-state Neutral conditions would shift the transition period between 06 June and 19 June, with 12 June as the seventh day.

Further study is needed to evaluate exact criteria for the onset dates pertaining to each special interest group, including special consideration for the growing season of Missouri crops and agricultural products, as well as special consideration for the summer tourism and entertainment season in the state. This might eventually lead to three different forecasted summer onset dates, one agricultural, one touristic and one meteorological, but separating the interests would likely provide a more valuable application of this study.

By examining 500-mb geopotential heights, the coupling effect of El Niño Southern Oscillation with Pacific Decadal Oscillation, mean daily temperature and maximum daily temperature data, along with the frequency of significant precipitation, a final onset date for summer was chosen for sixty-three years. This work will combine with the research done by Ratley et al. (2002) and Birk et al. (2010) to fill the void of localized information for the spring-to-summer transition in the state of Missouri. This knowledge, along with future studies, could aid the economic choices of agriculture, as well as provide safer guidance for people during a time where the atmosphere is changing its regime. This information will help both long-range forecasters and future models to identify the change of regime from spring to summer in the future.

## **Chapter 6 FURTHER STUDY**

A surprising revelation of this study concerned the basic category of mode, or the numerical value in a data set that presents itself most often, which may or may not be equal to the median or the mean (depending on the data set). Weather forecasters are instructed to not predict the same temperature two days in a row. In fact, logic often precludes repeating temperatures: there are too many atmospheric variables in constantly-shifting states to lead to the exact same maximum (or minimum) temperature prediction over a twenty-four-hour period. However, daily maximum temperature data from Jefferson City from 1948-2013 showed an intriguing number of same-temperature pairs and triplets throughout the May, June and July months. A climatology study on this area focusing on the reasoning for the heightened existence of maximum temperature modes would provide insight to future forecasters. In addition, an analysis of the mode of temperatures could itself become another parameter for summer onset dates, as the expectation for less variation in daily maximum temperatures increases with the commencement of summer.

Though the specific coupling of ENSO/PDO was the highlight of this research, teleconnections have shown that most planetary-scale oscillations have global impacts. It would be beneficial to look at these same data using the other identifiable oscillations as the basis of temperature and precipitation patterns,

including the Atlantic Multidecadal Oscillation (AMO) and the Quasi-Biennial Oscillation (QBO).

Finally, the information collected from this research could be further examined using the averages of 500-mb global geopotential heights as bases for energy surrogates in the Northern Hemisphere, as demonstrated by Ratley et al. (2002). The wave amplitude index shown by Ratley et al. (2002) illustrates that summations of waves decrease value with time throughout the course of one year, which would be another beneficial parameter to use with which to identify the change of spring (a time of higher wave activity) to summer (a time of decreasing wave activity and thus lower atmospheric energy).

## REFERENCES

- Ahrens, C. D. *Essentials of Meteorology*. CA: Cengage Learning, 2012. Print.
- "Annual Estimates of the Population for the United States, Regions, States, and Puerto Rico: April 1, 2010 to July 1, 2013" (CSV). *2013 Population*. Retrieved April 24, 2014.
- Bentley, M. L. and T. Mote, 1998. A Climatology of Derecho-Producing Mesoscale Convective Systems in the Central and Eastern United States, 1986-1995. Part I: Temporal and Spatial Distribution. *Bull. Amer. Meteor. Soc.*, **79**, 2527-2540.
- Birk, K., A. R. Lupo, P. Guinan and C.E. Barbieri, 2010. The Interannual Variability of Midwestern Temperatures and Precipitation as Related to the ENSO and PDO. *Atmósfera*, **23**, 95-128.
- Bove, M. C., J. B. Elsner, C. W. Landsea, X. Niu and J. J. O'Brien, 1998. Effects of El Niño on U.S. Landfalling Hurricanes, Revisited. *Bull. Am. Meteorological Soc.*, **79**, 2477-2482.
- Carleton, A. M., D. L. Arnold, D. J. Travis, S. Curran and J. O. Adegoke, 2008. Synoptic Circulation and Land Surface Influences on Convection in the Midwest U.S. "Corn Belt" During the Summers of 1999 and 2000. Part I: Composite Synoptic Environments. *J. Climate*, **21**, 3389-3415.  
doi: <http://dx.doi.org/10.1175/2007JCLI1578.1>
- "El Niño/Southern Oscillation (ENSO)." *El Niño/Southern Oscillation (ENSO)*. National Climatic Data Center, 2014. Web. 08 May 2014.
- Fasullo, J. and P. J. Webster, 2002. Hydrological Signatures Relating the Asian Summer Monsoon and ENSO. *J. Climate*, **15**, 3082-3095.
- Grimm, A. M. and R. G. Tedeschi, 2009. ENSO and Extreme Rainfall Events in South America. *J. Climate*, **22**, 1589-1609.
- Hanley, D. E., M. A. Bourassa, J. J. O'Brien, S. R. Smith and E. R. Spade, 2003. A Quantitative Evaluation of ENSO Indices. *J. Climate*, **16**, 1249-1258.  
doi: [http://dx.doi.org/10.1175/1520-0442\(2003\)16<1249:AQEOEI>2.0.CO;2](http://dx.doi.org/10.1175/1520-0442(2003)16<1249:AQEOEI>2.0.CO;2)
- Hart, R. E. and R. H. Grumm, 2001. Using Normalized Climatological Anomalies to Rank Synoptic-Scale Events Objectively. *Mon. Wea. Rev.*, **129**, 2426-2442. doi: [http://dx.doi.org/10.1175/1520-0493\(2001\)129<2426:UNCATR>2.0.CO;2](http://dx.doi.org/10.1175/1520-0493(2001)129<2426:UNCATR>2.0.CO;2)

- "Historical Records and Trends." *National Climatic Data Center (NCDC)*. National Oceanic and Atmospheric Administration, n.d. Web. 21 Apr. 2014.
- Huang, D., X. Ni, Q. Tang, X. Zhu and D. Xu, 2012. Spatial and Temporal Variability of Sea Surface Temperature in the Yellow Sea and East China Sea over the Past 141 Years. *Modern Climatology*, **7**, 213-234.
- Hu, Q. and S. Feng, 2012. AMO- and ENSO-Driven Summertime Circulation and Precipitation Variations in North America. *J. Climate*, **25**, 6477-6495.
- Hu, Z.-Z. and B. Huang, 2009. Interferential Impact of ENSO and PDO on Dry and Wet Conditions in the U.S. Great Plains. *J. Climate*, **19**, 5500-5518.
- Huff, F. A. and S. A. Changnon, 1986. Potential Urban Effects on Precipitation in the Winter and Transition Seasons at St. Louis, Missouri. *J. Climate Appl. Meteor.*, **25**, 1887-1907.
- "JMA SST ENSO Index." Center for Ocean-Atmospheric Prediction Studies, n.d. Web. 21 Apr. 2014.
- Kung, E. C. and J.-G. Chern, 1995. Prevailing Anomaly Patterns of Global Sea Surface Temperatures and Tropospheric Responses. *Atmósfera*, **8**, 99-114.
- Lorenz, E. N., 1963. The Mechanics of Vacillation. *Journal of Atmospheric Sciences*, **20**, 448-465.
- Lorenz, E. N., 1969. Atmospheric Predictability as Revealed by Naturally Occurring Analogues. *Journal of Atmospheric Sciences*, **26**, 636-646.
- Mantua, N. J., S. R. Hare, Y. Zhang, J. M. Wallace and R. C. Francis, 1997. A Pacific Interdecadal Climate Oscillation with Impacts on Salmon Production. *Bull. Am. Meteorol. Soc.*, **78**, 1069-1079.
- Minobe, S., 1997. A 50-70 Year Climatic Oscillation Over the North Pacific and North America. *Geophys. Res. Lett.*, **24**, 683-686.
- Mo, K. C., 2010. Interdecadal Modulation of the Impact of ENSO on Precipitation and Temperature over the United States. *J. Climate*, **23**, 3639-3656.
- "ModelAssist for ModelRisk." *ModelAssist for ModelRisk*. VOSE Software, n.d. Web. 14 May 2014.
- Muñoz, E., C. Wang and D. Enfield, 2010. The Intra-Americas Springtime Sea Surface Temperature Anomaly Dipole as a Fingerprint of Remote Influences. *J. Climate*, **23**, 43-56.

- "National Weather Service Weather Forecast Office." *Climatological Data for St. Louis, Columbia, and Quincy*. National Weather Service, n.d. Web. 21 Apr. 2014.
- Nese, J. M., R. G. Najjar and J. G. Murgo, 2012. Climate Science and the Broadcast Meteorologist. *Bull. Amer. Meteor. Soc.*, **93**, 1913–1916. doi: <http://dx.doi.org/10.1175/BAMS-D-12-00025.1>
- Palecki, M.A. and D. J. Leathers, 2000. Spatial Modes of Drought in the United States. *Preprints of the 12<sup>th</sup> Conference on Applied Climatology*, 8-11 May, 2000, Asheville, North Carolina.
- Pennesi, K., 2011. Making Forecasts Meaningful: Explanations of Problematic Predictions in Northeast Brazil. *Wea. Climate Soc.*, **3**, 90–105. doi: <http://dx.doi.org/10.1175/WCAS-D-10-05005.1>
- Peterson, T. C., 2003. Assessment of Urban Versus Rural in Situ Surface Temperatures in the Contiguous United States: No Difference Found. *J. Climate*, **16**, 2941–2959.
- Pielke, R. A. and C. N. Landsea, 1999. La Niña, El Niño and Atlantic Hurricane Damages in the United States. *Bull. Amer. Meteor. Soc.*, **80**, 2027–2033. doi: [http://dx.doi.org/10.1175/1520-0477\(1999\)080<2027:LNAENO>2.0.CO;2](http://dx.doi.org/10.1175/1520-0477(1999)080<2027:LNAENO>2.0.CO;2)
- Ratley, C. W., A. R. Lupo and M. A. Baxter, 2002. Determining the Spring to Summer Transition in the Missouri Ozarks using Synoptic Scale Data. *Transactions of the Missouri Academy of Sciences*, **36**, 55-62.
- Shinker, J. J. and P. J. Bartlein, 2009. Visualizing the Large-Scale Patterns of ENSO-Related Climate Anomalies in North America. *Earth Interactions*, **13**, 1-50.
- "Sir Gilbert Walker." *About Sir Gilbert Walker*. University of Reading, n.d. Web. 21 Apr. 2014.
- "Two-Way Tables and the Chi-Square Test." *Two-Way Tables and the Chi-Square Test*. Yale, n.d. Web. 13 May 2014.
- "U.S. Daily Weather Maps - NOAA Central Library." *U.S. Daily Weather Maps - NOAA Central Library*. National Oceanic and Atmospheric Administration, n.d. Web. 21 Apr. 2014.
- Wang, S.-Y., T.-C. Chen and J. Correia, 2009. Climatology of Summer Midtropospheric Perturbations in the U.S. Northern Plains. Part I: Influence on Northwest Flow Severe Weather Outbreaks. *Climate Dynamics*, **31**, 1221-1237.

Wu, R. and B. P. Kirtman, 2007. Roles of the Indian Ocean in the Australian Summer Monsoon–ENSO Relationship. *J. Climate*, **20**, 4768–4788.

“2013 Missouri Exports.” Missouri Department of Economic Development, Mar. 2013. Web. May 2013.

"50 State Rankings for Size." *50 States in Square Miles from NETSTATE.COM*. NSTATE, LLC, n.d. Web. 15 May 2014.